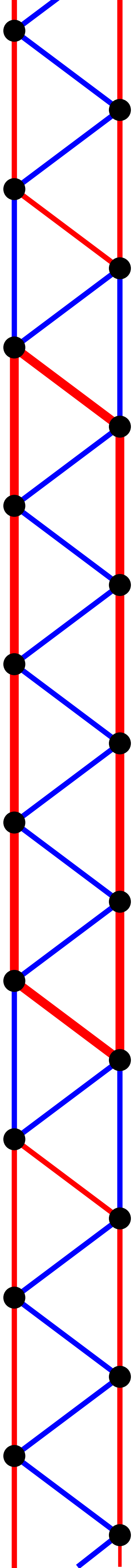

Parameters of Bar k-Visibility Graphs

Mareike Massow

Parameters of Bar k-Visibility Graphs

Diplomarbeit
bei Prof. Dr. S. Felsner

vorgelegt von Mareike Massow
am Fachbereich Mathematik der
Technischen Universität Berlin

Berlin, 19. Juli 2006

Die selbständige und eigenhändige Anfertigung versichere ich an Eides statt.

Berlin, 19. Juli 2006

Contents

Introduction

"The true mystery of the world is the visible, not the invisible."
Oscar Wilde

How can geometric settings be encoded combinatorially? Which discrete structures extract the essential information from continuous arrangements? How can the combinatorial properties of visibility arrangements in the plane be captured? Questions such as these are studied in computational geometry and geometric graph theory, two fundamental areas of modern discrete mathematics.

Although visibility in the plane is a very natural concept, many fundamental problems remain unsolved. Visibility graphs are a much studied approach to these problems. Generally speaking, a visibility graph consists of a set of shapes in the plane, the vertices, and a concept of visibility that defines the edges of the graph.

The presented diploma thesis provides answers to the initial questions posed for the class of bar k-visibility graphs. These graphs are a structure modeling some of the essential properties of visibility configurations. We will see that they carry a lot of structure, but their combinatorics can still be quite complex.

Bar visibility graphs are among the best understood classes of visibility graphs. Here the vertices correspond to horizontal line segments called *bars*, and visibility runs vertically along *lines of sight* which connect two bars while being disjoint from all others. These graphs have been completely characterized by Tamassia and Tollis [30] and independently by Wismath [33]. The concept of bar visibility graphs came up in the early 1980s when many new problems in visibility theory arised, originally inspired by applications dealing with determining visibilities between different electrical components (codeword 'VLSI-design'). Other applications arise when large graphs are to be displayed in a transparent way, and in the rapidly developing field of computer graphics.

Several variations and generalizations of bar visibility graphs have been considered, using different definitions for the type of bars or the kind of visibility or often both. For example, Bose, Dean, Hutchinson and Shermer [3] introduced rectangle visibility graphs, considering rectangles with horizontal and vertical visibility. Hutchinson [21] investigates arc- and circle-visibility graphs, where the vertices correspond to arcs of concentric circles and visibility can go through the origin. Recently, new classes of bar visibility have been introduced by restricting the vertex representations to unit bars [10] or generalizing them to sets of several bars [4].

Bar k-visibility graphs are another recent generalization of bar visibility graphs. They have been introduced by Dean, Evans, Gethner, Laison, Safari and Trotter [8] on the Graph Drawing Symposium 2005 in Limerick. The new idea is that lines of sight are allowed to intersect at most k other bars. This variation results in a much more complex class of graphs: While it is easy to see that all bar visibility graphs are planar, this is not true for bar k-visibility graphs, and no other immediate property provides an approach to their structure. To gain more insight into this graph class, Dean et al. are mostly interested in measuring how far a bar k-visibility G is from being planar. One method is to ask for a collection of planar subgraphs whose union is G. This is where the graph parameter *thickness* comes into play.

The (graph-theoretic) thickness of a graph G, denoted by $\theta(G)$, is the minimum number of planar subgraphs whose union is G. Thickness has been introduced by Tutte [31] in 1963. Mansfield [24] showed that determining the thickness of a graph is $\mathcal{NP}$-hard in general. Exact values are known for the complete graphs [1, 2], but only for very few other classes of graphs. For a survey on theoretical and practical aspects of thickness see [25].

Back to bar k-visibility graphs: For the case $k = 1$, Dean et al. [8] used the Four Color Theorem to show that their thickness is bounded by 4. They conjectured that no bar 1-visibility graph has thickness larger than 2. The main new result of this diploma thesis is the construction of a bar 1-visibility graph with thickness 3, disproving the conjecture of Dean et al. from [8]. We conjecture that 3 is the tight upper bound on the thickness of bar 1-visibility graphs.

Having shown that there are bar 1-visibility graphs with thickness 3, we attack the problem from the other side by asking if 2 is the correct upper bound for a subclass of bar 1-visibility graphs. We consider bars extending from the y-axis to the right, such bars are called *semi bars*. Semi bar 1-visibility graphs have thickness at most 2. We prove this by presenting an algorithm that partitions the edges of a given such graph into two planar subgraphs.

Semi bar k-visibility graphs are a graph class worth studying beyond the case $k = 1$. We will see that they provide a setting in which our initial questions can be answered effectively, as they can be encoded by a unique permutation of $[n]$. We use this encoding to solve a number of graph problems posed for the case of semi bar k-visibility graphs.

The two main new results of this diploma thesis are the construction of a bar 1-visibility graph with thickness 3 and the algorithm showing that semi bar 1-visibility graphs have thickness at most 2. They will be presented on the Graph

Drawing Symposium 2006 in Karlsruhe. The corresponding paper titled “Thickness of Bar 1-Visibility Graphs” [19] is to appear in the conference proceedings.

For the remainder of this introduction we turn to prerequisites and structure of this diploma thesis. The graphs we are dealing with are simple and undirected, unless explicitly stated otherwise. We assume basic graph theory concepts to be known. For terminology not defined here we refer to [12].

In Chapter 1, bar visibility graphs are introduced with the main earlier results and methods. In particular, we investigate different concepts of visibility and bar representations that have been considered in the literature. Chapter 2 introduces semi bar visibility graphs. We characterize these graphs and show how to reconstruct and count the semi bar visibility representations of a given abstract graph. Chapter 3 deals with bar k-visibility graphs. We present all previously known results and give a construction of a bar 1-visibility graph with thickness 3. In Chapter 4, semi bar k-visibility graphs are introduced. We show tight results for a number of graph parameters, and present the algorithm mentioned above dividing the edges of a semi bar 1-visibility graph into two planar graphs. Finally, stimuli for further research are given in the Conclusion.

Acknowledgements

I am grateful to all the people in Louisiana and Berlin who made me detect my love for graph theory.

In particular I thank my advisor Stefan Felsner for many inspirational hours he spent with me and beautiful mathematics. Thanks go to Ekkehard Köhler for his interest in my diploma thesis and for co-supervising it. I am also thankful to my proofreaders for their very valuable comments.

Special thanks go to Florian Zickfeld for sharing his literature from Limerick, his advice and his office.

I still and again wish to thank Christina Puhl for providing any support at any time.

Chapter 1

Bar Visibility Graphs

"Zieh den Balken aus Deinem Auge,
dann wirst Du klar sehen..."
Jesus von Nazareth

The first chapter of this diploma thesis provides an overview of the results on bar visibility graphs. In Section 1.1 we define bar visibility graphs and introduce the basic notations we need. We will consider several concepts of visibility in the following sections, starting with weak visibility in Section 1.2. The main result of the theory on bar visibility graphs, their complete characterization, is presented in Section 1.3. Finally in Section 1.4 we investigate a special case of bar representations.

1.1 Definition

Here is the basic definition of bar visibility graphs, which will be subject to variations and generalizations later on:

Definition 1.1. *A graph G is a* bar visibility graph *if it admits a* bar visibility representation *as follows: The vertices of G are represented by pairwise disjoint horizontal line segments, henceforth called* bars*, in the Euclidean plane. Two vertices are joined by an edge if and only if the two corresponding bars can be joined by a vertical line segment, called* line of sight*, which is disjoint from all other bars. In this case the two bars are* visible *to each other.*

Figure 1.1 shows an example of a bar visibility representation together with the graph it induces. This model was first introduced by Luccio et al. [22] in 1983. As mentioned before, several modifications of bar visibility graphs have been considered in the literature. Different concepts of visibility have been defined (see

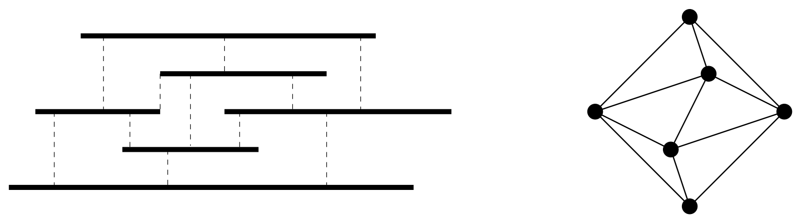

Figure 1.1: Example of a bar visibility representation, shown with the induced graph.

Section 1.3 and Section 1.2); the one introduced above is also called *strong visibility* if it needs to be distinguished from other models. Another way of varying the definition is to consider arbitrary intervals instead of segments, which are intervals closed at both endpoints. An overview of the different concepts of visibility graphs has been given by Tamassia and Tollis in their *Unified Approach to Visibility Representations of Planar Graphs* [30], with extensive references to the primal authors of each variant.

A first important property of bar visibility graphs can be observed immediately. Recall that a graph is *planar* if it can be drawn in the plane such that no two edges meet in a point other than a common vertex. A graph drawn in this way is *plane*, and the drawing is called a *planar embedding*. It is easy to construct a planar embedding of a bar visibility graph from a corresponding bar representation: We choose a line of sight for each visible pair of bars, shrink each bar to a point and bend lines of sight (which become edges) while maintaining adjacencies. Thus, all bar visibility graphs are planar.

In the remainder of this section, we introduce more notions and notations that we need to talk about bar visibility graphs. We denote vertices of the considered graphs with $u, v, w, \dots$ as usual. Referring to the corresponding bars we write $B(u), B(v), B(w)$. The set of bars representing a set V of vertices is denoted by $B(V)$. Whenever it is clear which kind of visibility (and, later on, which kind of bars) we are considering, we will say *bar representation* instead of bar visibility representation. Most of the time we carefully distinguish between vertices and the bars representing them; however, we will often adopt graph notions to bars, e.g., we say that two bars are *adjacent* or *neighbors* if the corresponding vertices are. In labelings of figures we will be a bit sloppy and denote a bar $B(v)$ with v. On the other hand we will use notions inspired by visibility: We say that two bars that can be joined by a line of sight in the considered model *see each other*.

Given a configuration of n bars, each bar is identified by three parameters: Its y-coordinate, the x-coordinate of its left endpoint, and the x-coordinate of its right endpoint. Thus we obtain three canonical ways to label the bars: Referring to the order of their left endpoints from left to right, we label them

$B(\ell_1), B(\ell_2), \dots B(\ell_n)$. Referring to the order of their right endpoints we label them $B(r_1), B(r_2), \dots B(r_n)$, this time enumerating from right to left. Thus, the vertex ℓ_1 corresponds to the bar with the leftmost left endpoint, and r_1 corresponds to the bar with the rightmost right endpoint. Finally, if we are interested in the order of the y-coordinates of the bars, we start with the topmost one and label the bars $B(t_1), B(t_2), \dots B(t_n)$.

In the following sections, we will consider different concepts of bar visibility graphs and their characterization.

1.2 Weak Visibility

When investigating the different variations of visibility graphs that have been introduced in earlier literature, we first encounter a concept with little demands on the graphs admitting a suitable bar representation; this variant is called *weak visibility*.

Definition 1.2. *A graph has a* weak bar visibility representation *if its vertices can be represented by bars such that bars corresponding to adjacent vertices can be joined by a vertical line segment disjoint from all other bars.*

Now a *weak bar visibility graph* is a graph admitting a weak bar visibility representation. Henceforth we will assume this relation whenever we define a new kind of bar visibility representation.

Weak visibility has been first considered in 1978 by Otten and van Wijk [26] who gave an algorithm for constructing a weak bar visibility representation of 2-connected planar graphs. Unaware of their result, a couple of years later Duchet et al. [14] showed by a simple and straightforward argument that any planar graph admits such a representation. Note that the converse is also true, that is, any weak bar visibility graph is planar. This can again be seen by the simple argconstruction used in the previous section for bar visibility graphs. Thus, the following theorem implies that the two graph classes, planar graphs and weak bar visibility graphs, coincide. We present the proof of Duchet et al. [14].

Theorem 1.3. *Every planar graph admits a weak bar visibility representation.*

Proof. Let $G = (V, E)$ be a planar graph with a corresponding straight-line embedding in the plane. Such an embedding exists by Fary's Theorem [17]. Now choose a direction different from the directions of all edges to be the horizontal direction. Replace each vertex by a horizontal line segment disjoint from all edges and all other vertices; this is clearly possible if the segments are chosen short enough (cf. Figure 1.2). Let us call the resulting representation of our graph $\mathcal{F}$, consisting of *vertex-segments* and *edge-segments*.

If all edge-segments in $\mathcal{F}$ are vertical, we are done. Otherwise choose an edge e that is not represented vertically. Then we observe (without going into details here) that there exists a pseudo-line $L \subseteq \mathbf{R}^2$ with the following properties:

- L meets any horizontal line of the plane in exactly one point.
- L contains the ends of the segment representing e.
- L does not meet $\mathcal{F}$ outside of vertex-segments.

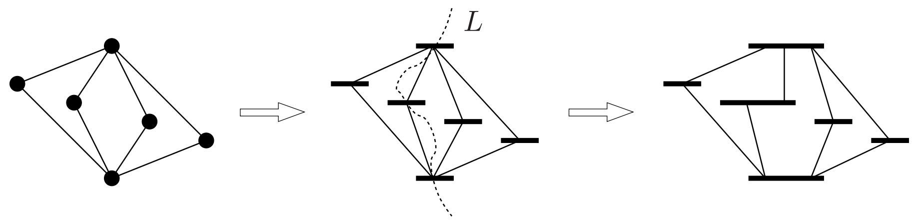

Figure 1.2: Constructing a weak visibility representation of a given plane graph with straight-line edges.

The pseudo-line L splits the plane into two parts which can be shifted apart horizontally without overlapping. A horizontal shifting about d extends the vertex-segments cut by L by the distance d. Now choose d large enough, then e can be replaced by a vertical line segment joining the two incident vertex-segments.

By repeating this procedure until all edge-segments are vertical we obtain the desired result. □

During the transformation of a graph into a weak bar visibility representation, some information gets lost: If we are only given the bars in the plane, they do not uniquely determine a graph with this bar representation. The concepts of visibility that we will consider in the following section (and in the rest of this diploma thesis) always require two bars to see each other if *and only if* the corresponding vertices are adjacent.

1.3 Characterization

The characterization of bar visibility graphs certainly is among the most satisfying results in the theory of visibility achieved so far. The main results of this section have been obtained independently by Tamassia and Tollis [30] and Wismath [33]. Here we sketch the ideas of Tamassia and Tollis; Wismath's proof of the characterization runs along similar lines.

As mentioned in Section 1.1, Tamassia and Tollis consider and compare different concepts of visibility in their paper [30]. The third variant besides strong and weak visibility is ε-visibility. The reconstruction of a bar ε-visibility representation of a given graph known to have one is easier than the corresponding task for strong visibility. Thus, Tamassia and Tollis first state a characterization of bar ε-visibility graphs. We will follow their path and then briefly sketch how this characterization can be extended to strong bar visibility graphs.

Definition 1.4. *A graph has a* bar ε-visibility representation *if its vertices can be represented by bars such that two vertices are adjacent if and only if the two corresponding bars can be joined by a vertical strip of non-zero width which is disjoint from all other bars.*

It is clear that given a configuration of bars, two ε-visible bars also see each other if strong visibility is considered. On the other hand, if there are bars $B(u)$ and $B(v)$ such that the right endpoint of the former has the same x-coordinate as the left endpoint of the latter, then they are neighbours in a strong visibility representation, but not in an ε-visibility representation (see Figure 1.3).

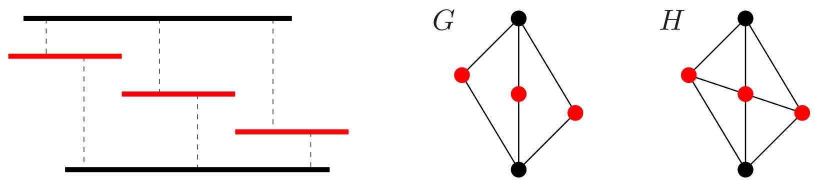

Figure 1.3: A bar ε-visibility representation of $G = K_{2,3}$. Strong visibility yields additional lines of sight between the red bars, inducing the graph H.

The following proposition forms the basis of the characterization of bar ε-visibility graphs. The proof is based on properties of s-t-numberings and bipolar orientations of graphs. We do not want to address these in detail here, and present only the ideas of the proof from [30].

Proposition 1.5. *Any* 2*-connected planar graph admits a bar* ε*-representation.*

Sketch of the proof. Tamassia and Tollis construct a bar ε-representation of a 2-connected planar graph $G = (V, E)$. As main tool making this possible they use *s-t-numberings*. An s-t-numbering of G, where s and t are distinct vertices in V, is a labeling σ of the vertices with $1, 2, \ldots, |V|$, such that $\sigma(s) = 1$, $\sigma(t) = |V|$, and each vertex $v \neq s, t$ has two neighbors u, w with $\sigma(u) < \sigma(v) < \sigma(w)$. Even and Tarjan [16] showed that for any 2-connected planar graph and every edge (s, t), an s-t-numbering can be found in linear time. Now, for a given 2-connected plane graph G, Tamassia and Tollis' idea is to compute an s-t-numbering σ of G and a corresponding numbering σ^* of its plane dual G^*. Directing the edges of G and

G^* from smaller to larger σ-numbers, we obtain a *bipolar orientation* of G and its dual counterpart, that is, we obtain acyclic orientations with unique source and sink. Properties of a bipolar orientation are e.g. that every face has a unique source and sink on its boundary, and the incoming and outgoing edges of every vertex appear consecutively in a cyclic order. We can use this last property to assign a unique left and right face to every vertex of G. This is all we need to compute the coordinates of the bar corresponding to a vertex v of G: The y-coordinate of the bar is given by the σ-number of v, and as x-coordinates for its left and right endpoint we use the σ^*-numbers of the left and right face of v. Tamassia and Tollis then show that this bar representation induces exactly the edges of G by further investigating properties and relations of the bipolar orientations of G and G^*. □

Tamassia and Tollis [30] now give a necessary condition for graphs with cut-vertices to have a bar ε-visibility representation. They can extend the construction of the previous proposition to all graphs fulfilling this condition, thereby completing the characterization of bar ε-visibility graphs.

Theorem 1.6. *A graph admits a bar ε-visibility representation if and only if it has a planar embedding such that all cutpoints are incident to the outer face.*

Proof. The necessity can be seen as follows: Let $\mathcal{B}$ be a bar ε-visibility representation of a graph G, and draw a vertical line-segment, i.e., an *edge-segment*, between bars that are ε-visible to each other. Construct a planar embedding $\hat{G}$ of G by shrinking each bar into a point and bending edge-segments such that adjacencies of vertices are maintained. Suppose for the sake of contradiction that in the resulting embedding there is a cut-vertex c of G which is not incident to the outer face. Then there are blocks $B_0, B_1, \ldots, B_j$ such that in $\hat{G}$ all blocks except B_0 lie entirely inside of an inner face of B_0, and any path from a vertex in B_i with $1 \leq i \leq j$ to a vertex in $\bar{G} = G \setminus \bigcup_{i=1}^{j} B_i$ passes through c. Consider the bars representing the blocks $B_1, \ldots, B_j$, and choose one of them (say, $B(v)$) that is topmost or bottommost among them in $\mathcal{B}$, but distinct from $B(c)$. The vertex v lies inside of an internal face of $\hat{G}$, hence it follows that $B(v)$ can be seen from a bar representing a vertex of $\bar{G}$. But then v is incident to a vertex of $\bar{G}$! This contradicts the fact that c is a cut-vertex.

To see that every graph with a planar embedding such that all cutpoints lie at the boundary of the outer face admits a bar ε-visibility representation, suppose that such a graph G and embedding are given. Then select the leaves from the block-cutpoint tree of G, that is, select all blocks of G that have only one cut-vertex in common with the rest of G. In any such block choose a vertex different from the cut-vertex. Now add a new vertex to the outer face and connect it to all the chosen vertices. The resulting graph is 2-connected and still planar. Thus, a bar ε-visibility representation of it can be computed by the previous proposition. The construction

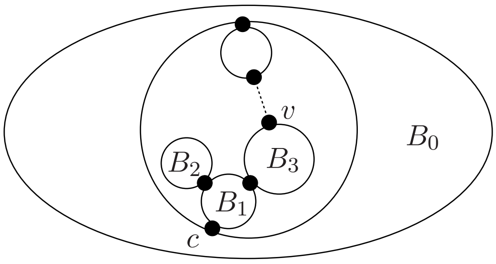

Figure 1.4: Arrangement of blocks in the proof of Theorem 1.6.

of the proof allows us to choose the topmost bar to represent the new vertex. Then by removing this segment we get an ε-visibility representation of G. □

We now have a complete characterization of bar ε-visibility graphs, but as ε-visibility is a restricted form of visibility, we are naturally interested in a similar result for strong visibility. First, it is easy to see that the necessary condition of Theorem 1.6 still holds, as an analogous proof to the one presented above can be used for strong visibility. Thus, any graph admitting a strong bar visibility representation has an embedding with all cut-vertices on the outer face. However, the converse is not true, and in fact there are even 2-connected planar graphs without strong bar visibility representation. The reason is that with ε-visibility, two bars can block the sight between a bar above them and a bar below them without being adjacent themselves (cf. Figure 1.3). Tamassia and Tollis [30] showed that if a 2-connected graph contains a vertex pair such that its removal separates the graph into more than three components, then this graph does not admit a strong bar visibility representation. Hence $K_{2,4}$ is an example of a bar ε-visibility graph which is not a strong bar visibility graph.

How can we see that in a strong bar visibility representation, a pair of bars can separate three components, but not four? Recall that Figure 1.3 showed a bar ε-visibility representation of $K_{2,3}$ which is not a strong bar visibility representation of this graph. However, $K_{2,3}$ does have a strong bar visibility representation, as shown Figure 1.5. This figure illustrates how three components can be separated in a strong bar visibility representation, and it provides an idea of what goes wrong for four. The proof of Tamassia and Tollis in [30] formalizes this idea.

Tamassia and Tollis also prove sufficient conditions for strong bar visibility graphs in [30]. They introduce *strong s-t-numberings* in which every inner face of the corresponding directed graph has to have an arc between its unique source and sink. Then they show that a 2-connected graph admits a strong bar visibility representation if and only if it has a strong s-t-numbering. For a general graph G, they define a 2-connected *s-t-extension* of G by adding two vertices s and t to G as well as edges connecting these two vertices to each other and to the rest of

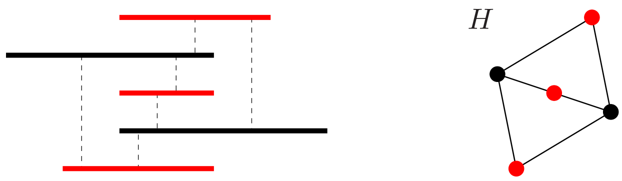

Figure 1.5: A strong bar visibility representation of $H = K_{2,3}$.

the graph. Now Tamassia and Tollis prove that strong bar visibility graphs are characterized as follows: A graph G has a strong bar visibility representation if and only if there is an s-t-extension of G admitting a strong s-t-numbering.

Given a strong bar visibility representation of a graph, we can easily turn it into a bar ε-visibility representation of the same graph by perturbing the endpoints of the bars a little bit. On the other hand, we know from the result of Tamassia and Tollis stated above that there are graphs admitting a bar ε-visibility representation but no strong bar visibility representation. We conclude that the class of strong bar visibility graphs is a proper subset of the class of bar ε-visibility graphs.

1.4 A Special Case: *x*-Different Bar Representations

In Section 1.1, we have noticed that in a bar visibility representation, each bar is identified by three parameters, and these parameters induce three natural ways to label the vertices of a bar visibility graph. We would like these labelings to be unique. Therefore, we try to perturb the x- and y-coordinates of the bars a little bit in the case that the t-, ℓ- and r-order are not unique.

As for the y-coordinates, this does not create a problem: Bars with the same y-coordinate form an independent set, and slightly pertubing the y-coordinates – without otherwise altering the vertical order of the bars – until they are pairwise different will neither create nor delete any lines of sight. Thus in the following we can assume the bars to have pairwise different y-coordinates.

The matter is more delicate when it comes to the x-coordinates of endpoints of bars. Perturbing the endpoints can create new lines of sight; this holds for ε-visibility as well as for strong visibility. Consider the bar representation of C_5 in Figure 1.6: No matter how we break the tie of equal abscissae of the right endpoints, we will necessarily introduce a chord and thus obtain a different graph.

Definition 1.7. *A bar visibility representation is* x-different *if the endpoints of its bars have pairwise different* x*-coordinates.*

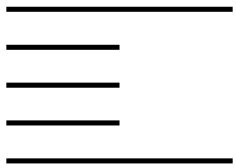

Figure 1.6: A bar visibility representation of C_5

Let us consider the class of graphs admitting an x-different bar visibility representation. First we can observe that the distinction between strong visibility and ε-visibility is obsolete here: If two bars see each other and no two of their endpoints have the same abscissa, then automatically they can be joined by a vertical strip of non-zero width disjoint from all other bars, thus, they are ε-visible. Since any two bars that are ε-visible already are strongly visible by definition, we see that the two concepts of visibility coincide for our restricted class of bar representations. Thus, we can safely speak of the class of x-different bar visibility graphs, without further specifying the kind of visibility.

The class of x-different bar visibility graphs has been studied by Luccio, Mazzone and Wong [23]. They obtained a characterization of this class, unaware that Tamassia and Tollis (cf. [30]) studied visibility graphs in such a similar setting. However, the results turn out to have a quite different flavor. For reconstructing a bar representation of a given graph, Luccio et al. use a detour via multigraphs: They define a planar multigraph to be *triangular* if it has an embedding in the plane such that all inner faces are bounded by 3-cycles. They call a simple graph *ipo-triangular* if it can be transformed into a triangular planar multigraph by successive duplication of existing edges. The main result of [23] now is the following:

Theorem 1.8. *A graph is an x-different bar visibility graph iff it is ipo-triangular.*

The necessity of the ipo-triangularity is not hard to see. Luccio et al. consider rectangular visibility zones defined by lines of sight. For any such visibility zone between two bars, they add an edge between the corresponding vertices. The resulting graph is a multigraph as there can be several visibility zones between two bars. Then if a vertical line is swept over an x-different bar representation one observes that any newly encountered bar forms a triangle with the two bars directly above and below (if they exist), see Figure 1.7. Similarly, if the right endpoint of a bar constitutes the ends of visibility zones to two bars directly above and directly below, a new visibility zone between these two bars begins, again inducing a 3-cycle. With this idea it can be seen that any inner face of the considered multigraph is bounded by a 3-cycle. For the other direction, Luccio et al. use a triangular embedding of a multigraph to construct an x-different bar representation. This is done by successively realizing the 3-faces. For the complete proof and the technical details of the construction see [23].

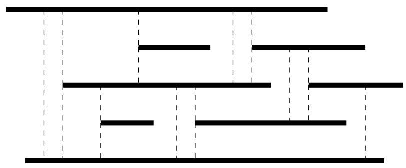

Figure 1.7: Any x-different bar representation induces an ipo-triangular graph.

Consider again the bar representation of Figure 1.6. We observed above that by slightly disturbing the endpoints we cannot turn it into an x-different bar visibility representation of C_5. Theorem 1.8 proves that there actually is no way of representing C_n for $n \geq 4$ with x-different bars, since clearly these graphs cannot be turned into triangular multigraphs by duplication of existing edges.

It follows that there are graphs having a strong bar visibility representation, but no x-different bar visibility representation. Thus we can conclude that the class of x-different bar visibility graphs is a proper subset of the class of strong bar visibility graphs. Recall that by the results of Section 1.3, the latter is in turn a proper subset of the class of bar ε-visibility graphs.

Note that considering only x-different bar representations is not a restriction if we are interested in the maximum number of edges of a bar visibility graph, or if we consider problems that only get harder with more edges, for example finding the chromatic number of a graph. This is justified by the fact that perturbing endpoints of bars that previously had the same abscissa may only yield new lines of sight, but can never block existing ones. We will need this in Section 3.2 where we make use of a unique ℓ- and r-order of the vertices.

In the next chapter we consider bar representations in which right endpoints of bars are x-different, whereas the left endpoints all have the same abscissa.

Chapter 2

Semi Bar Visibility Graphs

"Let's pick a graph out of a hat and see if we're lucky."
Graham Brightwell

We have seen in the last chapter that all bar visibility graphs are planar. In this chapter, we introduce a special case of bar visibility representations which restricts the class of the corresponding graphs to outerplanar graphs. We define this subclass of bar visibility graphs in Section 2.1. For a given maximal outerplanar graph with labeled Hamilton cycle, a bar representation inducing it can be constructed efficiently, as we will see in Section 2.2. There we also show a complete characterization of the considered subclass of bar visibility graphs. In Section 2.3 we will see how to explicitly count the number of different bar representations inducing the same maximal outerplanar graph with the fixed labeling of its Hamilton cycle.

2.1 Definition

In this section we define semi bar visibility graphs and see how they can be encoded by permutations.

Definition 2.1. Semi bars *are horizontal segments in the plane extending from the* y*-axis to the right.*
A graph is a semi bar visibility graph *if it has an* x*-different semi bar visibility representation, i.e., a bar visibility representation such that all left endpoints are at* $x = 0$ *and all right endpoints have pairwise different abscissae.*

We rotate semi bar visibility representations counterclockwise as shown in Figure 2.1; in the following we will always think of them in this way. If we talk about *bar representations* in this chapter, it is an abbreviation of x-different semi bar visibility representation.

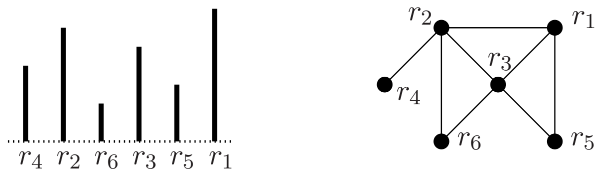

Figure 2.1: Example of a semi bar visibility graph with a corresponding bar representation.

In the previous chapter we considered strong visibility and ε-visibility between bars. Note that these two notions coincide here, as any two bars that see each other in the bar representations of this chapter do so over a line of sight of positive width. Now let a fixed bar representation be given. We define two unique orderings of the bars: Label the bars $B(r_1), B(r_2), \ldots, B(r_n)$ by decreasing y-coordinate of the upper endpoint. Thus, the r-order lists the semi bars by decreasing height. For the second permutation label the bars $B(t_1), B(t_2), \ldots, B(t_n)$ from left to right. The index of a vertex in the t-order (respectively r-order) is also called its *t-position* (respectively *r-position*). Note the different view on the r- and t-order compared to the last chapter, due to the rotation of the bar representation! The ℓ-order of the last chapter is useless in this setting.

With the above correspondence, two given permutations of $[n]$ together uniquely define a bar representation, and thus the graph induced by it. Now if we assume without restriction that the t-order is the natural order of the numbers 1 to n, then the graph is encoded by just one permutation of $[n]$. To get this permutation, we just have to read the r-labels of our bar representation from left to right. For example, the semi bar visibility graph of Figure 2.1 is encoded by the permutation $(4, 2, 6, 3, 5, 1)$. This permutation fixes the order of the height of the bars from left to right and thus completely determines the bar representation.

Without the assumption that the bar representation has to be x-different, semi bar visibility graphs have been defined by Cobos, Dana, Hurtado, Márquez and Mateos on the Graph Drawing Symposium 1995, see [6]. They investigate a classification of graphs (the *representation index*) with respect to the kind of visibility representation they admit, and introduce semi bar visibility representations as inducing the graphs of representation index $1 + 1/2$.

2.2 Characterization

In this section we characterize semi bar visibility graphs as graphs with an outerhamiltonian embedding in which all inner faces are triangles. This is defined in detail below.

We start with showing that any semi bar visibility graph is outerplanar. After that we reconstruct a bar representation for a maximal outerplanar graph G given with a labeling of its Hamilton cycle. Then we formulate under which conditions this construction can be extended to general outerplanar graphs. For constructing the bar representation, we make use of the dual tree of an embedded maximal outerplanar graph; a tool which will also help us in the next section to count the number of bar representations inducing G.

The first lemma also tells us how to obtain a planar straight-line drawing of a semi bar visibility graph given by a bar representation:

Lemma 2.2. *Every semi bar visibility graph is outerplanar.*

Proof. Let a semi bar visibility graph G be given by a corresponding bar representation. We will use this bar representation to define an outerplanar embedding of G. This can easily be done: Embed each vertex v at the upper endpoint of $B(v)$. Connect vertices corresponding to visible pairs of bars by a straight line. Figure 2.2 illustrates the embedding. This embedding is planar: If two edges $t_i t_k$ and $t_j t_\ell$ would cross, then necessarily we would have $i < j < k < l$. But the shortest of the four corresponding bars cannot see beyond any of the longer bars, thus it cannot have an incident edge contributing to the crossing – a contradiction. In addition we observe that all bars extend into the outer face of the embedding, and thus all vertices are incident to this face. Therefore the embedding is outerplanar. □

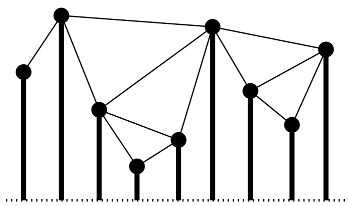

Figure 2.2: An outerplanar embedding of a semi bar visibility graph can easily be extracted from a bar representation.

Now instead of embedding a graph given by a semi bar visibility representation, we want to construct a bar representation of a given outerplanar graph. The main work is to achieve this for maximal outerplanar graphs. Let G be such a graph on n vertices, Figure 2.3 shows an example. For the construction we will use an outerplanar embedding of G. Let us briefly review some basic properties of such an embedding: It consists of an outer n-cycle and only triangular inner faces. Thus, G has a unique Hamilton cycle which contains exactly the edges incident to the outer face. Every such *outer edge* is contained in exactly one triangle (for $n \geq 4$), and every *inner edge* in exactly two. We have n outer edges, and $n - 3$ inner edges, which can be seen by triangulating the inner face of the n-cycle by a zig-zag path. It follows that there are $n-2$ inner triangles of G. Since the unique Hamilton cycle forms the boundary of the outer face in any outerplanar embedding of G, such an embedding is essentially unique.

As announced above, we will use the dual tree of G which is defined as follows:

Definition 2.3. *Let a maximal outerplanar graph G with outerplanar embedding be given. Let $C = t_1t_2 \dots t_n$ be a labeling of the Hamilton cycle of G in counterclockwise order. The* dual tree *T of G is defined as follows: For every inner triangle f of G, the tree T contains an inner vertex f^*. Two such vertices are adjacent if and only if the corresponding triangles share an edge. The vertex corresponding to the triangle containing t_1t_n is chosen as the* root *of T. Now, every other inner vertex f^* of T gets connected to a new leaf of T for every outer edge incident to f.*

Note that as G is outerplanar, T cannot contain a cycle. Furthermore, since every triangle has exactly three incident edges, T is a *rooted binary tree*. Figure 2.3 illustrates the definition.

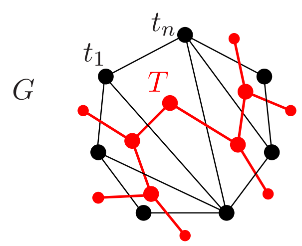

Figure 2.3: A maximal outerplanar graph G and its dual tree T.

Proposition 2.4. *For any maximal outerplanar graph G given with a labeled Hamilton cycle $C = t_1t_2 \dots t_n$, one can compute a semi bar visibility representation of G with the t-order prescribed by C.*

Proof. For $n \leq 2$, the assertion is trivial, thus let G have $n \geq 3$ vertices. Fix the outerplanar embedding of G in which C bounds the outer face in counterclockwise order. We will use properties of this embedding and the dual tree T of G to find a semi bar visibility representation of G.

The t-order of the bars is fixed by C. What remains to find out is the length of the bars, i.e., which t-position corresponds to which r-position. Since C is a closed cycle, $B(t_1)$ and $B(t_n)$ have to see each other and thus be the two longest bars, $B(r_1)$ and $B(r_2)$. Let us set $r_1 = t_1$ and $r_2 = t_n$. In each of the following steps we will determine the next longest bar while at the same time *realizing a triangle*, that is, fixing the r-position of its vertices and making sure that the bar representation we are constructing induces the edges of this triangle. Since there are $n-2$ bars left whose length we still have to specify, and there are also $n-2$ inner triangles of G, we will have realized every edge of G in the end.

First, choose as f_0 the unique triangle containing the outer edge t_1t_n, then f_0^* is the root of T. There is a unique vertex in G adjacent to both t_1 and t_n, say, t_i. On the other hand, there is a unique bar in any bar representation seeing both $B(t_1)$ and $B(t_n)$. Thus, we let $B(t_i)$ be the third longest bar in $\mathcal{B}$, i.e., we set $r_3 = t_i$. Now we have realized f_0, and to keep this in mind, we *mark* the corresponding vertex f_0^* of T.

Suppose that we have specified which t-position corresponds to $r_1, r_2, \ldots, r_p$, with $p \geq 3$. In each of the following steps, choose an unmarked inner vertex f^* of T which is adjacent to a marked one. Since T is a tree and the marked vertices always form a connected subgraph, it follows that f^* is adjacent to exactly one marked vertex in T. Choosing f^* corresponds to choosing a new triangle f adjacent to a triangle f' that is already realized. Let the three vertices of f be t_j, t_k, t_ℓ. By the choice of f^* we know that exactly one of the three edges of f is already realized, say, t_jt_ℓ. Assume without restriction that $j < \ell$. We claim that $j < k < l$. To see this, note that there are two t_j-t_ℓ-paths on C, one of them (let us call it P) contains t_1t_n. Since there must be a path of realized triangles from f' to f_0, the third vertex of f' must lie on P. But then the third vertex of f, which is t_k, must lie on the other path – and this is the path containing all t_m with $j \leq m \leq l$. Thus we have $j < k < l$ as claimed.

As t_j and t_ℓ belong to f' which has been realized before, the length of $B(t_j)$ and $B(t_\ell)$ is already fixed. Furthermore, the edge t_jt_ℓ is realized, i.e., there is a line of sight between $B(t_j)$ and $B(t_\ell)$, which means that no bar with a t-position inbetween them is longer. Now it is clear that $B(t_k)$ needs to be the longest bar between them, because then (and only then) the edges t_jt_k and $t_\ell t_k$ are realized. Therefore we set $r_{p+1} = t_k$. Then we have realized f and can mark f^* (see Figure 2.4 for an example).

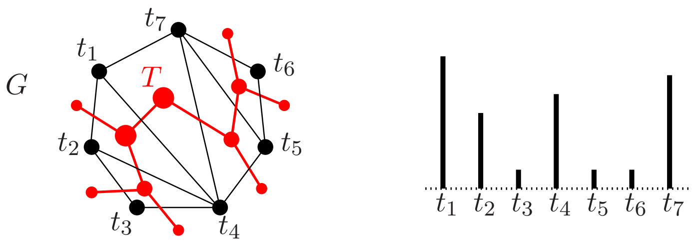

Figure 2.4: Constructing a bar representation: The longest bar between $B(t_1)$ and $B(t_4)$ has to be $B(t_2)$.

The bar representation $\mathcal{B}$ defined by the given t-order and the constructed r-order realizes the edge of every inner triangle, and thus every edge of the maximal outerplanar graph G. Furthermore, we have seen in Lemma 2.2 that every semi bar visibility representation induces an outerplanar graph. Therefore $\mathcal{B}$ cannot induce additional edges not contained in G. We conclude that $\mathcal{B}$ is a semi bar visibility representation of G. □

In the example of Figure 2.4, the longest four bars have been determined so far. Accordingly, two dual vertices are marked, and two triangles of G are already realized. The other bars do not yet have a determined length.

Now we can specify in which cases we can reconstruct a semi bar visibility representation of a general outerplanar graph, and thus prove the characterization of semi bar visibility graphs.

Definition 2.5. *A graph is* outerhamiltonian *if it has a Hamilton path P and a planar embedding such that all edges of P are incident to the outer face. Such an embedding is called an* outerhamiltonian embedding *with respect to P.*

Figure 2.5 shows an example of a graph G with an outerhamiltonian embedding with respect to a Hamilton path P. Note that this graph is not maximal outerplanar. The figure also shows the smallest example of an outerplanar graph which is not outerhamiltonian.

Figure 2.5: Examples: An outerhamiltonian graph G with Hamilton path P, and an outerplanar graph H which is not outerhamiltonian.

Theorem 2.6. *A graph G is a semi bar visibility graph if and only if it has an outerhamiltonian embedding in which all inner faces are triangles.*

Proof. Let us first take care of the necessity. We will show that for a semi bar visibility graph G given by a bar representation $\mathcal{B}$, the embedding described in the proof of Lemma 2.2 has the desired properties. Let us call an embedding obtained from $\mathcal{B}$ as specified in that proof *extracted from* $\mathcal{B}$. First it is clear that such an embedding is outerhamiltonian with respect to the Hamilton path $P = t_1t_2 \ldots t_n$ (cf. Figure 2.2). Now we show by induction on the number of bars (or vertices) that all inner faces of an extracted embedding are triangles. If $\mathcal{B}$ has at most three bars, this is obvious. Suppose that $\mathcal{B}$ has $n \geq 4$ bars and that any embedding extracted from a bar representation on lesser bars has only triangular inner faces. Choose the vertex r_n corresponding to the shortest bar in $\mathcal{B}$ and delete it. The resulting embedding is extracted from $\mathcal{B} \setminus B(r_n)$, and by the induction hypothesis all its inner faces are triangles. If $B(r_n)$ is the leftmost or the rightmost bar of $\mathcal{B}$, then the only edge incident to r_n is the one in P. Adding r_n with its incident edge to the outer face of the embedding extracted from $\mathcal{B} \setminus B(r_n)$ corresponds to reinserting $B(r_n)$ into $\mathcal{B}$ and then considering the embedding extracted from $\mathcal{B}$. Hereby no new inner faces are created. Now if $r_n = t_i$ with $2 \leq i \leq n-1$, then r_n has exactly two neighbors, t_{i-1} and t_{i+1}. In the embedding of $G \setminus r_n$ extracted from $\mathcal{B} \setminus B(r_n)$, the edge $t_{i-1}t_{i+1}$ is incident to the outer face. Thus we can insert $r_n = t_i$ into the outer face and connect it with its two neighbors, creating one new inner face, which is a triangle. The resulting embedding of G is exactly the embedding extracted from $\mathcal{B}$. We conclude that this embedding is outerhamiltonian with only triangular inner faces.

Now suppose that a plane graph G is given with a Hamiltonian path $P = t_1t_2 \dots t_n$ incident to the outer face, such that all inner faces are triangles. Add two vertices t_0 and t_{n+1} to the outer face, and close the Hamilton cycle $C = t_0t_1 \dots t_nt_{n+1}$ such that C is the boundary of the outer face. Triangulate the inner face incident to t_0t_{n+1}. The resulting graph G' clearly is maximal outerplanar. Note that the only edges of G' not contained in G are incident to t_0 or t_n. Figure 2.6 shows how the graph G from the previous figure is turned into a maximal outerplanar graph G'.

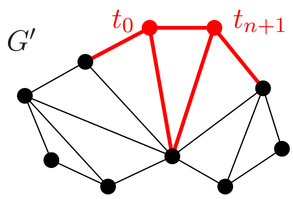

Figure 2.6: Making an outerhamiltonian graph maximal outerplanar by closing a Hamilton cycle with two new vertices and triangulating the new inner face.

Now construct a semi bar visibility representation $\mathcal{B}'$ of G' with the t-order of C as described in the proof of Proposition 2.4. All edges of G are realized in $\mathcal{B}'$, and as G' is maximal outerplanar, no additional edges between two bars $B(t_i)$ with $1 \leq i \leq n$ can be induced by $\mathcal{B}'$. Let $\mathcal{B}$ be obtained from $\mathcal{B}'$ by deleting $B(t_0)$ and $B(t_{n+1})$. Since $B(t_0)$ and $B(t_{n+1})$ are the leftmost and rightmost bar of $\mathcal{B}'$, deleting them does not yield any new lines of sight. The edges of G are still realized in $\mathcal{B}$. Thus, $\mathcal{B}$ is a semi bar visibility representation of G. □

In [6], Cobos et al. characterize graphs admitting a semi bar visibility representation (not necessarily x-different) as outerhamiltonian graphs. Their proof is different from ours, but we can observe that bars with the same length yield larger faces with four or more boundary vertices in the embedding extracted from a semi bar visibility representation.

2.3 Counting Bar Representations

We have seen above how we can construct a bar representation of a given maximal outerplanar graph, using its dual tree. Now even with the Hamilton cycle and the t-order of the vertices fixed, there are multiple bar representations inducing the same graph. The aim of this section is to find out explicitly how many.

In general, given a fixed t-order of n vertices, one can find $n!$ different bar representations by choosing a permutation of the length of the n bars, i.e., their r-order. We also know how many different maximal outerplanar graphs on n vertices with a fixed labeled Hamilton cycle there are: It is the number of triangulations of a convex n-gon, which is known to be the *Catalan number* C_{n-2}, where

$$C_n = \frac{1}{n+1}\binom{2n}{n}.$$

For a comprehensive collection of results and references concerning Catalan numbers see Stanley's book *Enumerative Combinatorics* [29]. Let us fix a particular maximal outerplanar graph G with a labeled Hamilton cycle C. The set of bar representations inducing G forms the class $\mathcal{C}_G$. Note that the cardinality of $\mathcal{C}_G$ varies, depending on the structure of G: If the inner vertices of the dual tree T of G build a path with the root as end-vertex, the bar representation inducing G is almost unique (the only freedom we have is reversing the order of the two longest bars). On the other hand, if these inner vertices form a more ramified tree, the cardinality of $\mathcal{C}_G$ can get much larger. The construction in the proof of Proposition 2.4 tells us that the exact number depends on the number of choices we have to realize the next triangle. The following theorem will make this more precise.

Recall that the dual tree T is a binary tree with a specified root. There is a canonical way of embedding T, placing the root as topmost vertex and the other vertices in levels below it. Since we have a fixed embedding of G (with C bounding the outer face in counterclockwise order), we can orient the inner triangles of G and thus uniquely define a left and a right child of each inner vertex of T. Thus we can speak of the left and the right branch below an inner vertex of T.

Theorem 2.7. *Let G be a maximal outerplanar graph given with a labeled Hamilton cycle $C = t_1 t_2 \ldots t_n$ for $n \geq 3$. Let T be the dual tree of G, and let $I(T)$ be the set of its inner nodes. For each $x \in I(T)$, let ℓ_x be the number of inner nodes in the left branch below x, and r_x the number of inner nodes in the right branch. We assign to x the weight*

$$w(x) := \binom{\ell_x + r_x}{\ell_x} = \binom{\ell_x + r_x}{r_x}.$$

Then the number of semi bar representations with the t-order fixed by C is

$$2 \cdot w(T) := 2 \cdot \prod_{x \in I(T)} w(x).$$

Proof. We prove the assertion by induction on the number of vertices of G, with the additional claim that the factor 2 in the formula accounts for the choice of $B(t_1)$ or $B(t_n)$ as longest bar. If $n = 3$, then the dual tree T has the root as only inner vertex, and it follows $2 \cdot w(T) = 2$. In this case, G is a triangle, thus we know that $B(t_2)$ has to be the shortest bar in any bar representation of G. We can choose $B(t_1)$ or $B(t_2)$ to be the longest bar. Therefore there are two possible bar representations of G, and we obtain the desired result.

Now let a graph G on $n \geq 4$ vertices as in the statement be given, and suppose that the theorem holds for any graph of smaller order. Consider the proof of Proposition 2.4: A bar representation is constructed by choosing an r-order of the vertices. Recall that there is a unique way of choosing the t-position of the third longest bar. This bar $B(r_3) = B(t_i)$ defines two ranges for the t-position of the shorter bars: They can be placed between $B(t_1)$ and $B(t_i)$ or between $B(t_i)$ and $B(t_n)$. There are no lines of sight between bars on different sides of $B(t_i)$. Thus, once we have fixed an "internal" r-order for the bars in the left range and respectively for the bars in the right range, we can choose the set of r-indices for the $i-2$ bars in the left range arbitrarily from $\{r_4, \ldots, r_n\}$.

After determining the t-position of the third longest bar, there are $n-3$ shorter bars left for which the t-position is still open. In the dual tree T, these correspond to $n-3$ unmarked inner nodes. It follows that we have $\ell_x + r_x = n - 3$ for the root x of T. Now let T' be the left branch below x, and let T'' be the right branch (cf. Figure 2.7).

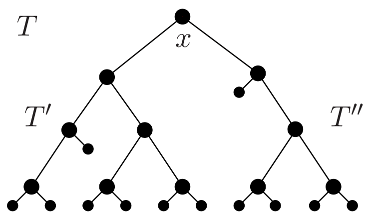

Figure 2.7: The root x contributes a weight of $\binom{10}{6}$ to the weight of the tree.

By the induction hypothesis, the number of permutations inducing $G[t_1, \ldots, t_i]$ with longest bar $B(t_1)$ is $w(T')$. Analogously, the number of permutations inducing $G[t_i, \ldots, t_n]$ with $B(t_n)$ as longest bar is $w(T'')$. Thus for any choice of ℓ_x shorter bars which are to be placed left of $B(t_i)$, we can calculate the number of 'legal' permutations of their length, in the sense that they constitute a part of a bar representation of G with the given t-order. Then the number of permutations of the $n-3$ bars shorter than $B(t_i)$ realizing all edges of G is

$$\binom{\ell_x + r_x}{\ell_x} \cdot w(T') \cdot w(T'') = w(x) \cdot w(T') \cdot w(T'') = w(T)\,.$$

To get the total number of bar representations of G (with the fixed t-order), we have to multiply the result by 2 again since we can choose $B(t_1)$ or $B(t_n)$ as longest bar.

□

We get back to representations formed by semi bars in Chapter 4, where we consider a generalized form of visibility called k-visibility. The results of that chapter will also imply results on semi bar visibility graphs. For example, we will see a different way of reconstructing bar representations from a given abstract graph. We will also see results on the chromatic number, the maximum number of edges and the connectivity of bar visibility graphs.

Chapter 3

Bar *k*-Visibility Graphs

"That's the problem of finding hay in a haystack:
Each time you search it's another needle coming out."
Nati Linial

In this chapter we present the class of visibility graphs which is in the focus of this diploma thesis. Bar k-visibility graphs (BkVs) generalize the notion of bar visibility graphs, and they provide a concept interpolating between bar visibility graphs and interval graphs, as we will see. The following sections provide a state-of-the-art overview of bar k-visibility graphs: All results on BkVs that I am aware of are stated and proved here. Most of these results spring from two papers: Alice M. Dean, William Evans, Ellen Gethner, Joshua D. Laison, Mohammad Ali Safari and William T. Trotter introduced bar k-visibility graphs in [8] and on the Graph Drawing Symposium 2005 in Limericks. A short version of their paper is published in the Graph Drawing Proceedings, see [9]. Stephen G. Hartke, Jennifer Vandenbussche and Paul Wenger proved further results on bar k-visibility graphs which can be found in [20].

Each section in this chapter deals with one aspect of bar k-visibility graphs. We start with defining bar k-visibility graphs in Section 3.1. In Section 3.2 we show a tight bound for their maximum number of edges. This bound will yield an upper bound for the chromatic number in the third section of this chapter. In Section 3.4, we will see that the classes of bar k-visibility graphs for different k are not comparable under inclusion. The next two sections deal with constellations impossible for BkVs: We will see in Section 3.5 that for small d, the only d-regular BkVs are the complete graphs; and we will examine forbidden subgraphs of BkVs. In Section 3.7 we present an upper bound on the thickness of BkVs, first for general k and, improving on this, for the special case $k = 1$. The last section of this chapter contains the main new result of this diploma thesis: Improving the lower bound on the maximal thickness of bar k-visibility graphs we show that there is a bar 1-visibility graph with thickness 3. This disproves a conjecture of Dean et al. [8].

3.1 Definition

Recall the definition of bar visibility representations from Chapter 1. Imagining the bars of a this model as material bars in space, equipped with some kind of visibility sense, they are completely opaque: Each bar only sees the next one below (or above) it, and all lines of sight to even lower (or higher) bars are blocked. Now, thinking of the bars as being more and more transparent, we obtain the notion of bar k-visibility graphs.

Definition 3.1. *A graph is a* bar k-visibility graph *if it admits a* bar k-visibility representation *as follows: Each vertex is represented by a horizontal segment (*bar*) in the Euclidean plane. Two vertices are joined by an edge if and only if the two corresponding bars can be joined by a vertical line segment (*line of sight*), which intersects at most k other bars.*
Lines of sight that do not intersect any bar are called direct*, all others are* indirect lines of sight*. Inspired by this, the corresponding edges are divided into* direct and indirect edges*.*

Figure 3.1 shows an example of a bar 1-visibility representation with the induced B1V. The special case $k = 1$ will receive more attention later.

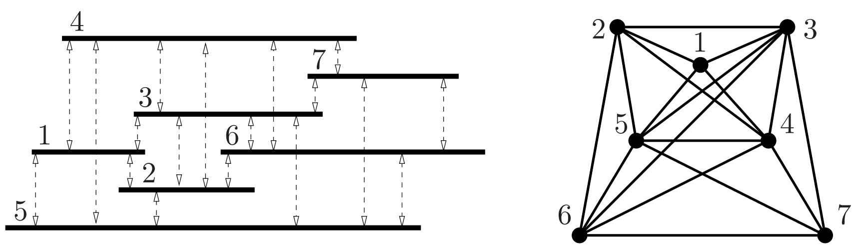

Figure 3.1: Example of a bar 1-visibility graph

In the following we will again say *bar representation* instead of *bar k-visibility representation* if it is clear which k-visibility is meant. Note that in our definition of BkVs, we allow lines of sight to have zero width.

When considering BkVs for the case $k = 0$, we are back in the setting of Chapter 1: B0Vs are exactly bar visibility graphs. The other extreme, $k = \infty$, yields another known class of graphs, namely, the interval graphs. Interval graphs are graphs that admit a representation of their vertices as closed intervals on the real line, such that two vertices are adjacent iff the corresponding intervals have a non-empty intersection. Projecting all bars on the real line we see that any graph admitting a bar ∞-visibility representation is an interval graph, and vice versa. In this way BkVs interpolate between bar visibility graphs and interval graphs. This correspondence will motivate results later in this chapter.

3.2 Maximum Number of Edges

As a first result on bar k-visibility graphs, we show a tight upper bound on the number of edges in this section. Some arguments in the proof already give a taste of what can or cannot happen in a BkV – and the result will prove to be useful often later on.

The following edge bound was shown in [20] by Hartke et al., after having been conjectured by Dean et al. who also proved several weaker results in [8]. The proof used by Hartke et al. and presented here refines an edge counting technique introduced by Dean et al. in a proof of their conjecture for the case $k = 1$.

Note that in this section we consider only x-different bar representations, i.e., we assume that endpoints of bars in a given bar representation have pairwise different x-coordinates. Recall that we observed in Section 1.1 that this is not a restriction since we are interested in the maximum number of edges. The advantage is that in the setting of x-different bar representations, the ℓ-, r- and t-order of the bars and the corresponding vertices are unique.

Theorem 3.2. *If $G = (V, E)$ is a bar k-visibility graph on $n > 2k + 2$ vertices with $k \geq 0$, then G has at most $(k + 1)(3n - 4k - 6)$ edges.*

Proof. Consider a fixed bar k-visibility representation of G, this induces an ℓ-, r- and t-order of the vertices. We count the edges by sweeping a vertical line over the representation, from left to right; each edge is counted as a *new edge* at the earliest appearance of the corresponding line of sight. Figure 3.2 illustrates the situation.

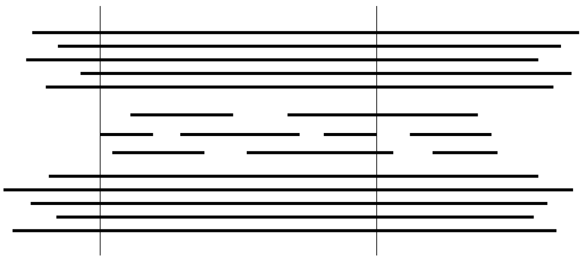

Figure 3.2: Passing a left endpoint, the sweep line can meet at most $2(k + 1)$ new lines of sight. At a right endpoint there are at most $k + 1$.

When the left endpoint of a bar $B(\ell_i)$ is encountered, at most $2(k + 1)$ new lines of sight can be created: Clearly every new edge is incident to ℓ_i, and $B(\ell_i)$ can see at most $k + 1$ bars above and $k + 1$ bars below. But the full number of new edges can only be created for $i > 2k + 2$; at the first $2k + 2$ left endpoints, we have at most $i - 1$ new lines of sight.

When sweeping the right endpoint of a bar $B(r_j)$, new lines of sight between bars above and below may appear: At most $k + 1$ bars above $B(r_j)$ now have the possibility to each see one new bar below $B(r_j)$. Thus, if $j > 2k+2$, we can have $k+1$ new bars. For j between $2k+2$ and $k+3$, the potential number of new edges at a right endpoint goes down from k to 1, decreasing by 1 in each step. The bars $B(r_{k+2}), B(r_{k+1}), \ldots, B(r_1)$ all see each other, so no new lines of sight are created when $k+2 \geq j \geq 1$.

In total, the sweep argument yields an upper bound of

$$\sum_{i=1}^{2k+2}(i-1) + \sum_{i=2k+3}^{n}(2k+2) + \sum_{j=2k+3}^{n}(k+1) + \sum_{j=1}^{k} j\,,$$

which simplifies already quite nicely to

$$\begin{aligned} & (k+1)(2k+1) + 2(k+1)(n-2k-2) + (k+1)(n-2k-2) + \tfrac{1}{2}k(k+1) \\ = \; & (k+1)(3n - \tfrac{7}{2}k - 5)\,. \end{aligned}$$

This upper bound was shown in [8] already. By examining the bar representation more carefully, we detect that we have overcounted some edges and hence can refine the bound. The upper bound above can only be obtained if a bar starts with $k+1$ other bars above and below as soon as possible, and a bar ends with $k+1$ bars above and below as long as this is possible. In other words, we would need to have equality for the following sets:

$$\begin{aligned} & \{t_1, t_2, \ldots, t_{k+1}\} \cup \{t_{n-k}, t_{n-k+1}, \ldots, t_n\} \\ & = \{\ell_1, l_2, \ldots, \ell_{2k+2}\} \\ & = \{r_{n-2k-1}, r_{n-2k}, \ldots, r_n\} \end{aligned}$$

But then we would have double-counted the $(k+1)^2$ edges between the topmost $k+1$ bars (the *top-bars*) and the bottommost $k+1$ bars (the *bottom-bars*): We first counted them at their left endpoint and for a second time when enough bars between them ended.

Let us investigate in detail what happens if the sets above are not equal. If we have a top-bar $B(t_i)$ which is not among the first $2k+2$ bars of the ℓ-order, then it does not contribute $2k+2$ new edges but only at most $k+1+i-1$. Similarly, if $t_i = r_j$ for $j \leq n-2k-2$, then at most $i-1$ bars above it can gain visibility when it ends. The same holds if $B(t_i)$ is a bottom-bar. We will use these facts for refining our edge count.

Let p be the number of top-bars which belong to both of the sets $\{\ell_1, \ell_2, \ldots, \ell_{2k+2}\}$ and $\{r_1, r_2, \ldots, r_{2k+2}\}$. Similarly, let q be the number of bottom-bars belonging to the same two sets. We have observed above that we double-counted the pq edges between these bars.

The remaining $k+1-p$ top-bars begin among the last $n-(2k+2)$ bars or end among the first $n-(2k+2)$ ones (or both), therefore, their left or their right endpoint does not contribute the maximum number of edges. If $B(t_i)$ begins late or ends early, we overcounted $k+2-i$ edges, and thus lose the least possible edges if these $k+1-p$ bars represent $t_{k+1}, t_k, \ldots, t_{p+1}$. In this case, our first edge bound counted at least $1+2+\ldots+(k+1-p) = \frac{1}{2}(k+1-p)(k+2-p)$ too many edges. In the same way we counted at least $\frac{1}{2}(k+1-q)(k+2-q)$ too many edges at the bottom-bars.

Thus, our improved bound on the number of edges is

$$(k+1)\left(3n-\frac{7}{2}k-5\right) - pq - \frac{1}{2}(k+1-p)(k+2-p) + \frac{1}{2}(k+1-q)(k+2-q)\ .$$

Therefore we want to minimize the following function:

$$f(p,q) = pq + \frac{1}{2}(k+1-p)(k+2-p) + \frac{1}{2}(k+1-q)(k+2-q)$$

Note that f is symmetric in p and q. The partial derivatives of f both are $p+q-k-\frac{3}{2}$, thus, local extrema occur when $p = k+\frac{3}{2}-q$. Checking the second partial derivatives tells us that the function is convex, therefore it suffices to calculate $f(a, k+\frac{3}{2}-a)$ to find the minimum objective value of f. This yields $f(p,q) \geq \frac{1}{2}k^2 + \frac{3}{2}k + \frac{7}{8}$, and our upper bound becomes

$$(k+1)\left(3n-\frac{7}{2}k-5\right) - \left(\frac{1}{2}k^2+\frac{3}{2}k+\frac{7}{8}\right) = 3nk+3n-4k^2-10k-\frac{47}{8}\ .$$

Since the number of edges is an integer, we deduce that bar k-visibility graphs have at most $3nk+3n-2k^2-10k-6 = (k+1)(3n-4k-6)$ edges. □

We will see in an instant that the edge bound of the theorem can be attained. First let us harvest some fruits of our effort. Figure 3.3 shows a bar k-visibility representation of K_{4k+4}. With our edge bound it is now just a matter of counting to show that this is the largest complete BkV.

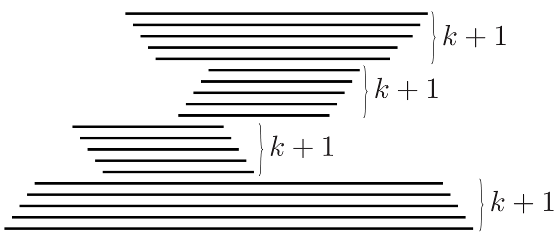

Figure 3.3: A bar representation of K_{4k+4}. This is an example of a BkV with the maximum number of edges.

Corollary 3.3. *If K_n is a bar k-visibility graph for $k \geq 0$, then $n \leq 4k+4$.*

Proof. Let us set $n = 4k+4+c$. Then the number of edges of K_n is

$$\frac{1}{2}(4k+4+c)(4k+4+c-1) = 8k^2 + 14k + 4ck + \frac{7}{2}c + \frac{1}{2}c^2 + 6\,.$$

From Theorem 3.2 we know that a BkV on $4k+4+c$ vertices has at most

$$(k+1)(3(4k+4+c) - 4k - 6) = 8k^2 + 14k + 3ck + 3c + 6$$

edges. Thus if K_n has a bar representation, we must have

$$\begin{array}{rrcl} & 4ck + \frac{7}{2}c + \frac{1}{2}c^2 & \leq & 3ck + 3c \\ \Longrightarrow & ck + \frac{1}{2}(c + c^2) & \leq & 0\,, \end{array}$$

which yields $c \leq 0$. Hence $n \leq 4k+4$.

□

Consider once again Figure 3.3. This complete graph has

$$\binom{4k+4}{2} = \frac{1}{2}(4k+4)(4k+3) = (k+1)(8k+6) = (k+1)(3n-4k-6)$$

edges. Thus, the upper bound of Theorem 3.2 is tight for $n = 4k+4$. To see that it is also tight for all larger n, insert arbitrarily many new bars between the two upper and the two lower packages of bars in Figure 3.3. This can be done such that the new bars each have $3(k+1)$ neighbors, and the number of neighbors of each old bar stays the same. Hence for every $n \geq 4k+4$ there is a BkV on n vertices with $(k+1)(3n-4k-6) = 3(k+1)n - (k+1)(4k+6)$ edges. For all smaller n, the complete graph is a BkV: Just leave out an arbitrary set of bars in Figure 3.3 to get a bar representation of K_n. Therefore, the tight upper bound on the number of edges in a BkV on $n \leq 4k+4$ vertices is given by $\binom{n}{2} = \frac{1}{2}n(n-1)$.

3.3 Chromatic Number

Recall that the chromatic number of a graph G is the smallest number k such that the vertices of G can be colored with k colors, assigning different colors to adjacent vertices. The chromatic number of a clique is obviously equal to the number of its vertices. We have seen in the previous section that K_{4k+4} is a bar k-visibility graph for any $k \geq 0$. Thus, $4k+4$ is a lower bound on the largest chromatic number of BkVs. The next proposition, taken from [8], provides an upper bound which follows from the maximum number of edges in a BkV.

Proposition 3.4. *Any bar k-visibility graph has chromatic number at most $6k+6$.*

Proof. The proof is done by induction on the number of vertices. Let $G = (V, E)$ be a BkV on n vertices and with m edges. The statement is trivial for $n \leq 6k + 6$. Let us assume that $n > 6k + 6$ and that the assertion holds for all smaller n. Theorem 3.2 now tells us that G has at most $(k + 1)(3n - 4k - 6)$ edges, and for its average degree it follows

$$d(G) = \frac{\sum_{v \in V} d(v)}{n} = \frac{2m}{n} \leq \frac{6n(k+1) - 2(4k+6)(k+1)}{n} < 6k + 6\,.$$

Thus, G has a vertex v of degree at most $6k+5$. Consider the graph $G \setminus v$. It might not be a BkV, but it is a subgraph of the BkV G' induced by a bar representation of G in which we have deleted $B(v)$. We can apply the induction hypothesis to see that $\chi(G') \leq 6k + 6$. Since G' only differs from $G \setminus v$ by (possibly) some additional edges, we also know that $\chi(G \setminus v) \leq 6k + 6$. Now it is easy to reinsert v and color it with a color not used by its neighbors. □

3.4 Comparing classes of bar *k*-visibility graphs

Now we are aiming to compare the classes of bar k-visibility graphs for different k. Let $\mathcal{F}_k$ denote the class of all BkVs. How does it differ from $\mathcal{F}_{k-1}$? We know from Section 3.2 that K_{4k+4} is a bar k-visibility graph, but no bar $(k-1)$-visibility graph, thus, $\mathcal{F}_k \not\subseteq \mathcal{F}_{k-1}$. Theorem 3.7 states that the reverse inclusion does not hold either. Thus $\mathcal{F}_k$ and $\mathcal{F}_{k-1}$ are incomparable under inclusion. The results of this section are among the further results on BkVs from [20].

The following simple lemma (simple to prove, that is – it takes more work to state it) will be useful for the proof of the main result of this section:

Lemma 3.5. *Suppose that for $k \geq 0$ in a bar representation of a BkV $G = (V, E)$ there are two vertices v, w such that $vw \notin E$, but there is a vertical line ℓ intersecting the two corresponding bars $B(v)$ and $B(w)$. Then any bar crossed by ℓ is contained in a $(k+2)$-clique consisting of bars intersected by ℓ as well.*

Proof. Because $B(v)$ and $B(w)$ do not see each other, there must be $k + 1$ bars blocking the sight, thus, any vertical line ℓ intersecting our two bars intersects at least $k + 3$ bars in total. Furthermore, any set of $k + 2$ vertically consecutive bars on ℓ forms a clique. □

Define an *n-wheel* W_n^k for $k > 0$ to be the graph formed by joining every vertex of a k-clique to every vertex of an n-cycle. Figure 3.4 shows a schematic drawing of the 6-wheel W_6^k.

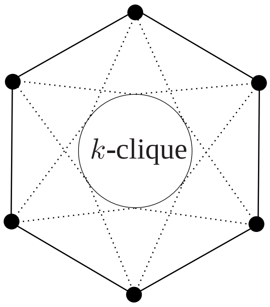

Figure 3.4: Scheme of the 6-wheel W_6^k.

Proposition 3.6. *W_n^k is not a bar k-visibility graph, for $n > 3$ and $k > 0$.*

Proof. Assume that there is a bar k-visibility representation of $W_n^k = (V, E)$ for some fixed k and $n > 3$. Let K denote the k-clique contained in W_n^k, and C the cycle. As W_n^k contains an induced (chordless) cycle of length greater than 3, it is not an interval graph. Thus, there are two bars $B(v)$ and $B(w)$ in our bar representation which intersect the same vertical line but do not see each other. From the lemma above it follows that v and w each are contained in a $(k+2)$-clique which necessarily also contains K. But the k bars in $B(K)$ do not suffice to block the sight between $B(v)$ and $B(w)$ – thus, there has to be at least one more bar of $B(C)$ between our two bars. Let $B(x)$ be such a bar and assume by symmetry that there are at most $k/2$ bars between $B(x)$ and $B(v)$. Then we have $x, v, w \in C$. Since $vw \in E$ we know that v and x appear consecutively on the cycle.

Let v' be the other neighbor of v on C. Then $v' \neq w$ (as $vw \notin E$) and $v'x \notin E$. There can be no $k + 1$ bars blocking the sight between $B(v')$ and $B(x)$, thus, there is a vertical band separating these two bars. Note that $B(v)$ traverses this vertical band. But since $W_n^k \setminus K \setminus v$ still leaves a connected graph, there has to be at least one more bar from C traversing this vertical band. Then necessarily there is such a bar visible from $B(v)$ – which is a contradiction since v has no more neighbors on C. □

The above proof closely follows the lines of the original proof presented in [20]; note, however, that Hartke et al. assumed $n \geq 5$ in the statement.

Figure 3.5 shows a construction of a bar ($k-1$)-visibility representation of W_n^k for large n and positive k. We have thus shown the following theorem:

Theorem 3.7. *For all $k > 0$, $\mathcal{F}_k$ and $\mathcal{F}_{k-1}$ are incomparable under inclusion.*

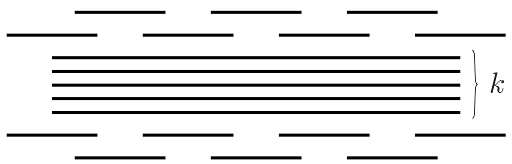

Figure 3.5: A bar $(k-1)$-visibility representation of W_n^k.

3.5 Regular Bar *k*-Visibility Graphs

Many of the results of Hartke et al. [20] are motivated by the question how the structure of interval graphs (which we observed to be bar ∞-graphs) can be transferred to bar k-visibility graphs. Since the only regular connected interval graphs are complete, they wondered if this remains true for bar k-visibility graphs. For small k, the answer is affirmative, as the following proposition shows. The proof presented here uses the same idea but a slightly different way of argumenting than the original one in [20]

Proposition 3.8. *If G is a connected d-regular bar k-visibility graph with $d \leq 2k+1$, then G is complete.*

Proof. Let G be a BkV as in the statement of the proposition, and fix a corresponding bar representation. Let $B(v)$ be a bar among those having the rightmost left endpoint. Let a be a vertical line containing the left endpoint of $B(v)$, and let $B(V_a) = \{B(a_1), B(a_2), \ldots, B(a_s)\}$ be the bars intersected by a (see Figure 3.6). Note that $v = a_i$ for some i. Then it holds $s \leq 2k+2$, for otherwise, a_{k+2} could see at least $k+1$ bars above and $k+1$ bars below and we would have $d = \deg(a_{k+2}) \geq 2k+2$, a contradiction. But now $\deg(a_{\lfloor s/2 \rfloor}) \geq s-1$ and $\deg(v) \leq s-1$, therefore, $d = s-1$.

If G is not complete, then there are two bars in $B(V_a)$ not seeing each other, and therefore, there is at least one bar ending left of a. Let b be the vertical line containing the last right endpoint left of a, and let $B(V_b) = \{B(b_1), B(b_2), \ldots, B(b_t)\}$ contain the bars with right endpoint on b. Note that there is no bar ending between b and a, and therefore, only bars in $B(V_a)$ can start in this (closed) vertical band.

G is connected, thus, there is at least one bar in $B(V_a)$ extending left such as to traverse b. Let $B(V_a') \subset B(V_a)$ be the set of such bars. Choose a bar which is 'central' in $B(V_a')$, more precisely, choose a_j in V_a' such that $|s/2-j|$ is minimized. Then in $B(V_a)$ and hence also in $B(V_a')$ there are at most $k+1$ bars above as well as below $B(a_j)$. We claim that $\deg(a_j) \geq s$.

We know already that $B(a_j)$ can see all bars in $B(V_a')$, thus, that a_j is adjacent to all vertices of V_a'. Furthermore, as the vertices in $V_a \setminus V_a'$ only have neighbors in V_a – their corresponding bars do not traverse b – we necessarily have that these

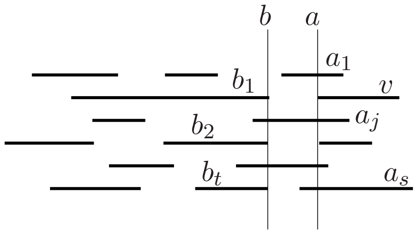

Figure 3.6: Illustration of the proof of Proposition 3.8.

vertices need to be adjacent to *all* $a_i \in V_a$ in order to have degree $s-1$. Now it follows that a_j is adjacent to these vertices, too, and hence to all $s-1$ vertices in V_a, and in addition to some vertex of V_b. Therefore, $\deg(a_j) \geq s$, which is a contradiction to G being $(s-1)$-regular. We conclude that G is complete. □

The natural question posed next is whether there are d-regular BkVs for $d \geq 2k+2$ which are connected but not complete. Hartke, Vandenbussche and Wenger started to answer this question in [20] by finding bar representations of connected d-regular non-cliques for $k \in \{0,1,2,3,4\}$ and $d = 2k+2$.

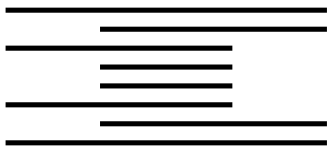

Figure 3.7: A bar 2-visibility representation of a 6-regular graph.

Figure 3.7 shows a bar representation of a 6-regular bar 2-visibility graph, which is formed by removing a perfect matching from K_8. It is not difficult to find bar representations of a similar type for a 4-regular B1V (K_6 without a matching) and a 2-regular B0V (K_4 without a matching, i.e., C_4). For $k=4$ and $d=10$, the bar representation in Figure 3.8 shows an example which can be used to construct an infinite class of 10-regular B4Vs: Just copy the middle section and insert it an arbitrary number of times.

The question whether connected d-regular bar k-visibility graphs which are not cliques exist remains open for larger values of d and k.

3.6 Forbidden Subgraphs

From the famous graph minor theorem of Robertson and Seymour it follows that if P is a graph property closed under taking minors, then the graphs fulfilling P

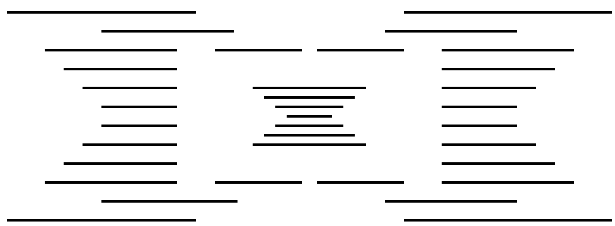

Figure 3.8: A bar 4-visibility representation of a 10-regular graph.

can be a characterized by a finite set of forbidden minors. For an introduction into the graph minor theorem, including a (naturally *very* rough, but at least providing the taste of an idea) sketch of the proof, see Chapter 12 of Diestel's newly edited book on Graph Theory [12]. The best known example is probably the forbidden set $\{K_5, K_{3,3}\}$ which by Kuratowski's Theorem (see Chapter 4 of [12]) characterizes the planar graphs.

Now the property of having a bar k-visibility representation is not closed under taking minors. This can be seen easily by adding a chain of short bars into a bar representation of K_{4k+4} (cf. Figure 3.3) such that the short bars together see all other bars, but do not block any line of sight. Then by contracting the chain to a single vertex we obtain K_{4k+5} which by Corollary 3.3 is not a BkV. However, forbidden substructures are still a promising approach to understand more about the structure of our graphs.

Hartke, Vandenbussche and Wenger found some forbidden subgraphs of BkVs in [20]. We present their results in this section.

Proposition 3.9. *Let H be a triangle-free graph which has no bar 0-visibility representation. Then no bar k-visibility graph contains H as an induced subgraph.*

Proof. Suppose a BkV $G = (V, E)$ contains an induced subgraph $H = (W, F)$ which is not a bar 0-visibility graph. Consider a fixed bar representation of G and the set of bars $B(W)$ representing H. Since H is not a bar 0-visibility graph, any bar representation of it contains an indirect edge.

Let $u, v \in W$ such that xy is an indirect edge of H and $B(w)$ is a bar traversed by the corresponding line of sight. Then necessarily $w \in W$ for at least one such w, else $B(W)$ would be a bar 0-visibility representation of H. But now $B(u)$ and $B(v)$ can both see $B(w)$ directly, and together with the edge uv this yields a triangle in H. □

Since all bar 0-visibility graphs are planar (see Chapter 1.3), we immediately have the following corollary:

Corollary 3.10. *A bar k-visibility graph does not contain a triangle-free non-planar induced subgraph.*

Another approach to the question posed in this section is to look at forbidden subgraphs of interval graphs. It is known that interval graphs do not contain the complete bipartite graph $K_{1,3}$ with each edge subdivided once as an induced subgraph. One may wonder whether similar structures are also forbidden in bar k-visibility graphs.

However, a simple construction shows that every tree T (and thus in particular the subdivided $K_{1,3}$) is an induced subgraph of a bar k-visibility graph for any $k \geq 0$. The idea is to choose a vertex r of T as root and partition the other vertices of T into levels according to their distance from r. Then one can build a bar representation of T inductively by first placing $B(r)$ on top. Having placed bars corresponding to the vertices of level i, one subdivides any such bar regarding the number of its children, and places shorter bars corresponding to those children below the bar. A k-clique between any two level of bars ensures that visibility only occurs between adjacent levels. See Figure 3.9 for an illustration of this construction.

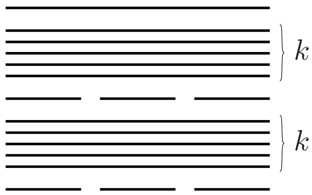

Figure 3.9: A BkV containing the subdivided $K_{1,3}$ as subgraph.

We have seen in this section that triangle-free non-planar graphs are not induced subgraphs of BkVs, but arbitrary trees are. Hartke et al. [20] ask for further characterization of BkVs by forbidden subgraphs – but so far, this is all we know.

3.7 Upper Bounds on the Thickness

We have seen in Section 3.3 that K_{4k+4} is a bar k-visibility graph, thus, for any $k > 0$, non-planar BkVs exist. We would like to know how nasty their non-planarity can get; therefore we seek to measure the closeness to planarity of BkVs. One parameter expressing this is the *thickness*, counting the minimum number of planar subgraphs of a graph. For the precise definition we refer to the Introduction chapter.

In this section, we present upper bounds on the thickness of BkVs. These results were shown by Dean et al. in the first paper on bar k-visibility graphs [8].

The case $k = 1$ will receive special attention as the Four Color Theorem yields the quite pleasing upper bound of 4 on the thickness of B1Vs.

Before looking more closely at the thickness of our graphs, we present a drawing induced by the bar representation of a given BkV. This drawing is not planar in general, but it will assist us with defining a coloring of the edges with not too many colors, such that every color class forms a plane graph.

3.7.1 2-Bend Drawing

Let G be a bar k-visibility graph given with a corresponding bar representation $\mathcal{B}$. We will use $\mathcal{B}$ to define a drawing of G in which each edge is a polyline with exactly two bends, a so-called 2-*bend drawing*. Figure 3.10 shows a 2-bend drawing of a BkV, extracted from a given bar representation.

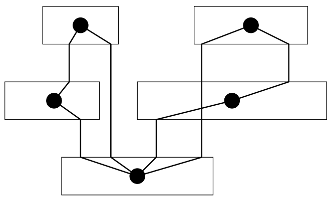

Figure 3.10: The 2-bend drawing of a graph extracted from a bar representation.

One can construct such a 2-bend drawing as follows: In a first step, enlarge each bar $B(v) \in \mathcal{B}$ until it is a rectangle with positive area. Choose a point in the interior of $B(v)$ to embed the vertex v, e.g., its center. If there is a (direct or indirect) line of sight between two bars, choose a vertical line segment connecting the two rectangles, not crossing other rectangles if the line of sight was direct. Each chosen line segment will constitute the *vertical part* of the corresponding edge. We choose the vertical line segments such that no two of them overlap. To make things easier, we also assume that the x-coordinate of any vertex differs from the x-coordinates of the vertical line segments corresponding to its incident edges. Clearly, such a choice of line segments is always possible. Now let an edge $e = uv$ consist of the vertical line segment representing the corresponding line of sight and the two non-vertical line segments joining its ends to u and v. Then e is drawn by a polyline with two bends.

Note that by our choice of the vertical line segments, crossings can only appear inside of a bar $B(v)$. Since edges incident to v do not cross, all crossings involve the vertical part of an edge traversing $B(v)$ and the non-vertical part of an edge incident to v.

3.7.2 A Bound for General *k*

With the above preparation, we can state the upper bound on the thickness θ of bar k-visibility graphs without further ado:

Theorem 3.11. *If G is a bar k-visibility graph, then $\theta(G) \leq 3k(6k+1)$.*

Proof. Consider a bar representation $\mathcal{B}$ of $G = (V, E)$ and a 2-bend drawing extracted from $\mathcal{B}$. Recall that $\mathcal{B}$ induces a bar ℓ-visibility graph for any $\ell \geq 0$; for $\ell = k-1$ let the corresponding graph be denoted by G_{k-1}.

The vertices in $V = V(G_{k-1})$ can be colored with $\chi(G_{k-1})$ colors such that no two vertices adjacent in G_{k-1} obtain the same color. We will use such a coloring C to define a coloring of E with the property that monochromatic edges do not cross in our 2-bend drawing of G.

In the 2-bend drawing, the vertical part of an edge $e = uv$ traverses at most k bars. The vertices corresponding to the traversed bars are pairwise adjacent also in G_{k-1}, thus, they all have different colors in C. If any line of sight corresponding to e traverses exactly k bars, then u and v are not adjacent in G_{k-1}, therefore these two vertices might have received the same color. We define an edge coloring as follows: If u and v have the colors c_1 and c_2 in C, then $e = uv$ receives the color $\{c_1, c_2\}$ (possibly consisting of just one element).

Suppose e crosses an edge f which has the color $\{d_1, d_2\}$; we need to show that $\{d_1, d_2\} \neq \{c_1, c_2\}$. Without loss of generality we may assume that e accounts for the vertical part of the crossing, thus, e traverses a bar corresponding to one of the end-vertices of f. This end-vertex is adjacent to u and v and therefore has a color different from c_1 and c_2. Hence $\{d_1, d_2\} \neq \{c_1, c_2\}$ and each color class of our edge coloring induces a plane graph in the 2-bend drawing.

Now $\theta(G)$ is bounded by the number of colors we used:

$$\theta(G) \leq \chi(G_{k-1}) + \binom{\chi(G_{k-1})}{2} = \chi(G_{k-1}) + \frac{1}{2}\chi(G_{k-1})\left(\chi(G_{k-1}) - 1\right)$$

From Proposition 3.4 we deduce that $\chi(G_{k-1}) \leq 6k$, whence we conclude $\chi(G_k) \leq 6k + 3k(6k-1) = 3k(6k+1)$. □

The edge bound given in the theorem above corrects a minor mistake in the original proof of [8], where the slightly lower upper bound of $2k(9k-1)$ was stated.

3.7.3 An Improved Bound for $k = 1$

For the special case of bar 1-visibility graphs, Theorem 3.11 shows that their thickness is bounded by 21. This bound can be considerably improved using the fact that bar 0-visibility graphs are planar. The powerful tool used here is the Four Color Theorem, which states that any planar graph has chromatic number at most 4. It has been first proven by Appel and Haken in 1977. The interested reader might prefer consulting the shorter proof given by Robertson, Sanders, Seymour and Thomas in [27].

Theorem 3.12. *Bar* 1*-visibility graphs have thickness at most* 4*.*

Proof. Given a B1V G with bar representation $\mathcal{B}$, we consider a 2-bend drawing of G as in the last proof. The bar visibility graph G_0 induced by $\mathcal{B}$ is planar. Let a proper 4-coloring of its vertices (and thus of $\mathcal{B}$) be given, the existence is guaranteed by the Four Color Theorem. With its help we will define a 4-edge-coloring of G such that each color class induces a plane graph.

The coloring rule is very simple: Any indirect edge receives the color of the bar it traverses; any direct edge receives a color different from the color(s) of its end-vertices. In this way we can obtain an edge-coloring using no more than the four colors of our vertex-coloring.

Consider an indirect edge $e = uv$, which corresponds to a line of sight traversing $B(w)$. The two bars $B(u)$ and $B(v)$ both have a direct line of sight to $B(w)$, thus, in the vertex-coloring of G_0 the vertex w is colored differently from the u and v. It follows that indirect edges as well never have the same color as their incident vertices.

Let e and f be two crossing edges such that the vertical part of e crosses a non-vertical part of f, i.e., $e = uv$ traverses a bar representing an end-vertex w of f. Suppose w is colored mauve, then by our coloring rule, e will be mauve, too – but since f is incident to w, it has a different color. Thus, monochromatic edges do not cross and G is the union of at most four planar graphs. □

We know that there are bar 1-visibility graphs with thickness greater than 1, and we just proved that it cannot be larger than 4. What, then, is the tight upper bound for the thickness of B1Vs: 2, 3 or 4?

We still do not have a final answer to this question. Dean et al. [8] conjectured that it is 2. We can say a little more now. We disprove their conjecture in the following section by constructing an SB1V with thickness 3.

3.8 A Bar 1-Visibility Graph with Thickness 3

In the previous section we investigated upper bounds for the thickness of bar k-visibility graphs. Now to estimate the quality of these upper bounds, we are looking for lower bounds on the maximal thickness of BkVs: What is the largest thickness we know that BkVs actually attain? So far we cannot say more than what follows from the existence of non-planar B1Vs: There are BkVs with thickness at least $k + 1$. Dean et al. asked if this is already the correct upper bound for the thickness of BkVs. In particular, they conjectured that bar 1-visibility graphs have thickness at most 2. In this section we construct a B1V with thickness 3, disproving their conjecture. Note that this construction yields an x-different bar representation.

We will often talk about a 2-*coloring* of a graph $G = (V, E)$, meaning a 2-coloring of the edges such that each color class is the edge set of a planar graph on V. Given a 2-coloring with blue and red we define G_{blue} and G_{red} as the graphs on V with all blue and all red edges, respectively.

Here is a brief outline of the construction: First we analyze a quite simple type of graph which has thickness 2 but with the property that every 2-coloring has uniform substructures, so called lampions. Assuming that the original graph is large enough we can assume arbitrarily large lampions. In a second step we introduce a series of slight perturbations into the original graph. It is shown that most of these perturbations have to be incorporated into lampions and the number of perturbations in one lampion is proportional to its size. However a lampion can only absorb a constant number of the perturbations. This yields a contradiction to the assumption that a 2-coloring exists.

Imagine an Autobahn where someone has heaped up the median strip, then consider the bar representation of the graph A_n shown in Figure 3.11. This graph has four special vertices A, B, C, D and a set V_{inner} of n inner vertices.

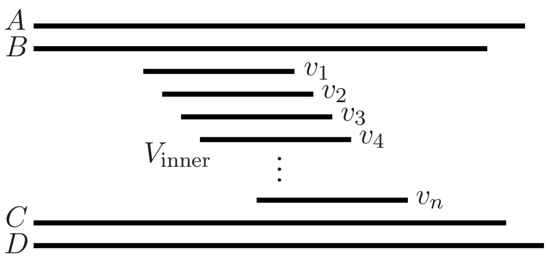

Figure 3.11: The Autobahn-graph A_n.

Since A_n contains a $K_{4,n}$ as subgraph we know that A_n is non-planar (assuming $n \geq 3$), hence, $\theta(A_n) \geq 2$. To show that $\theta(A_n) = 2$ we let G_{blue} consist of all direct edges and G_{red} consist of all indirect edges. Figure 3.12 shows the partition.

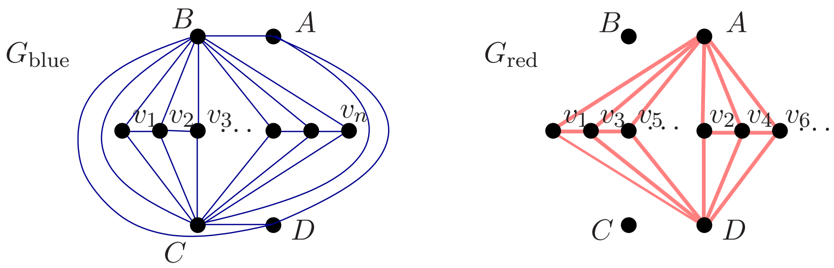

Figure 3.12: A partition of A_n into two planar graphs.

Let $V_{\text{inner}} = \{v_1, v_2, \ldots, v_n\}$, such that the indices represent the order of the right endpoints of the bars from left to right. The inner neighbors of v_i are $v_{i-2}, v_{i-1}, v_{i+1}$ and v_{i+2}. The graph $G[V_{\text{inner}}]$ induced by the inner vertices is maximal outerplanar with an interior zig-zag.

A *lampion* in a 2-coloring of A_n consists of a set $W = \{v_i, v_{i+1}, \ldots v_j\}$ of consecutive inner vertices and a partition $\{S_1, S_2\}$, $\{S_3, S_4\}$ of the four special vertices A, B, C, D such that G_{blue} consists of all zig-zag edges of $G[W]$ and all edges connecting vertices from W with S_1 and S_2, while G_{red} consist of the two outer paths of $G[W]$ and all edges connecting vertices from W with S_3 and S_4 (of course exchanging red and blue again yields a lampion). The set W is the *core of the lampion*. Thus, Figure 3.12 shows a lampion with core V_{inner} together with the additional edges between the four special vertices.

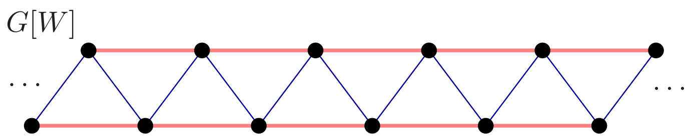

Figure 3.13: A lampion coloring of $G[W]$.

Lemma 3.13. *For every $k \in \mathbb{N}$ there is an $n \in \mathbb{N}$ such that in every 2-coloring of A_n there is a $W \subset V_{\text{inner}}$ with $|W| \geq k$ where W is the core of a lampion.*

Proof. Each inner vertex has four outer neighbors. Let us call an edge connecting an inner and an outer vertex a *transversal edge*. Consider the blue transversal edges; at each vertex there can be $0, 1, 2, 3$ or 4 of them. But G_{blue} is planar and therefore does not contain a $K_{3,3}$. Thus, at most two inner vertices can have the same three outer neighbors in G_{blue}. There are $\binom{4}{3} = 4$ different triples of outer neighbors in G_{blue}, so there can be at most eight inner vertices with more than two outer neighbors in G_{blue}. We might find another eight in G_{red}. These irregular vertices break the sequence $v_1, v_2, v_3, \ldots, v_n$ of inner vertices of A_n into at most 17 pieces, we remain with a 2-coloring of $A_{n'}$ with $n' \geq (n-16)/17$ such that all inner vertices are incident to exactly two blue and two red transversal edges.

Considering only the blue transversal edges of $A_{n'}$, the resulting subgraph G'_{blue} is a subgraph of a blown-up K_4 as illustrated in Figure 3.14. This subgraph is not arbitrary but has the property that every inner vertex has exactly two incident edges.

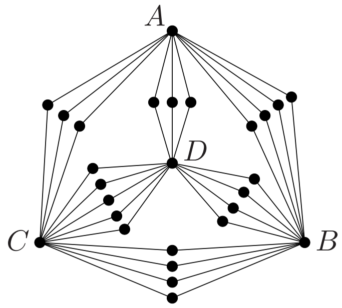

Figure 3.14: Blown-up K_4.

Now it remains to planarly embed the *inner edges* of $A_{n'}$, i.e. those of $G[V'_{\text{inner}}]$. To our disposition we have the ≤ 4 'large faces' of the blown-up K_4, which makes eight faces in total for the two planar graphs. In each of these faces we can embed at most three inner edges. There are other cases with fewer large faces which have in turn more inner vertices at the boundary. In all cases it is impossible to embed more than 12 edges between inner vertices with different outer neighbors in G'_{blue}. The red subgraph may contain another 12 irregular edges. These at most 24 irregularities break the sequence of inner vertices of $A_{n'}$ into at most 25 pieces, we remain with a 2-coloring of $A_{n''}$ with $n'' \geq (n' - 24)/25$ such that all inner vertices are incident to the same two special vertices in G'_{blue} and to the other two special vertices in G'_{red}.

We now have $K_{2,n''}$ as a subgraph in both G''_{blue} and in G''_{red}. The good thing about this is that $K_{2,n''}$ has an (essentially) unique planar embedding. Consequences for the inner edges of $A_{n'}$ are exploited in the following facts.

Fact 1**.** Every inner vertex of $A_{n''}$ has at most two incident inner edges of each color.

It follows that the 2-coloring of $A_{n''}$ induces a 2-coloring of $G[V''_{\text{inner}}]$ such that each color consists of a set of paths and cycles.

Fact 2**.** The set of blue inner edges of $A_{n''}$ contains at most one cycle. The same holds for the red inner edges. If there is a monochromatic cycle, then it is a spanning cycle of V''_{inner}.

There is not much freedom for a 2-coloring of the inner edges of $A_{n''}$ with these properties: We almost have a lampion coloring on $G[V''_{\text{inner}}]$. The exception is that there can be a single *Z-structure* (see Figure 3.15) in one color.

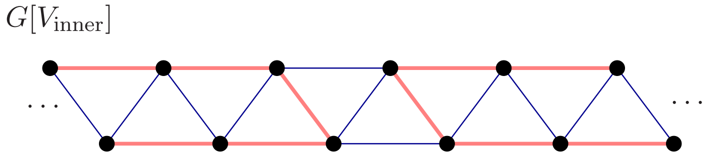

Figure 3.15: One Z-structure and no monochromatic cycle force all other edge-colors.

Removing the Z-structure leaves two consecutive pieces of the sequence of inner vertices. These pieces of V''_{inner} have a lampion coloring. The size of the larger piece can be estimated as $n''' \geq (n'' - 4)/2$. This proves the lemma. □

Well-prepared we can now look at the variant B_n of A_n in which we have slightly perturbed some of the inner bars. Figure 3.16 shows the result.

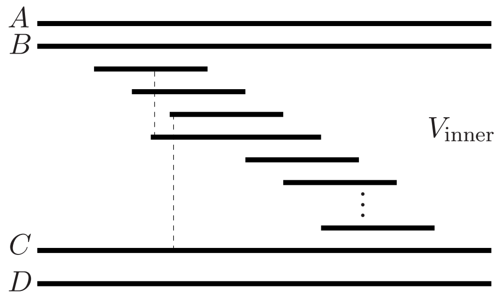

Figure 3.16: The perturbed Autobahn-graph B_n.

To get B_n, we have elongated every (say) tenth inner bar by pulling its left endpoint to the left, such that it is further left than the left endpoint of the bar directly above. With this modification we introduce an additional edge between the elongated bar $B(v_i)$ and $B(v_{i-3})$, but in turn we lose the edge between the bar v_{i+1} and the lowest special bar $B(D)$. Let us call the vertices corresponding to the elongated bars *modified vertices*.

Theorem 3.14. *The graph B_n is a bar 1-visibility graph with thickness 3, for n large enough.*

Proof. We will show that B_n has no 2-coloring. It follows that its thickness is at least 3, and since we can easily use a 2-coloring of A_n and embed the independent additional edges in a third graph, B_3 has thickness exactly 3. – Assume that B_n admits a 2-coloring. We first show that any 2-coloring of B_n would have to be very much alike a 2-coloring of A_n.

The vertices corresponding to a bar directly above a modified one – let us call them *reduced* – have only three outer neighbors. To avoid a $K_{3,3}$ in one color there can be at most 16 inner vertices incident to more than two transversal edges. In particular, most reduced vertices have to divide their three incident transversal edges into two of one color and one of the other. As in the proof of the lemma we consider a continuous piece in the sequence of inner vertices such that all inner vertices have at most two transversal edges of each color. The graph induced by the largest of these pieces and the special vertices is $B_{n'}$.

The blue subgraph G'_{blue} of $B_{n'}$ is a subgraph of a blown-up K_4 where at least $9/10$ of the inner vertices have degree 2 and the remaining reduced vertices have degree 1. As in the proof of the lemma it can be argued that there is only a constant number c of edges in G'_{blue} which join two inner vertices such that there are at least three different outer neighbours of these two vertices, i.e., which join two inner vertices which not belonging to the same blown-up edge of K_4. The constant can be bounded as $c \leq 24$. The red graph may contribute another set of c irregular edges. Removing the irregularities will break the sequence of inner vertices into at most $2c + 1$ pieces. The graph induced by the largest of these pieces and the special vertices is $B_{n''}$. Assuming that the edges between inner vertices and D are blue in the 2-coloring of $B_{n''}$ the transversal edges of G''_{blue} and G''_{red} are shown in Figure 3.17.

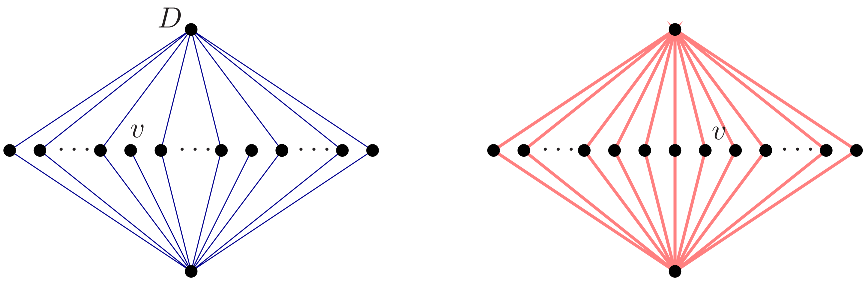

Figure 3.17: Embedding of a reduced vertex v in G''_{blue} and G''_{red}.

Let $v = v_{i-1}$ be a reduced vertex, the neighbors v_i and v_{i-3} of v both have inner degree 5. In G''_{red} they have degree (at most) 2, hence, they must have degree 3 in G''_{blue}. This is only possible if v_i, v_{i-1} and v_{i-3} form a blue triangle. Since v_{i-1} can have no further blue inner neighbors it follows that the edges $v_{i-1}v_{i-2}$ and $v_{i-1}v_{i+1}$ must be red, i.e., we have the situation shown in Figure 3.18.

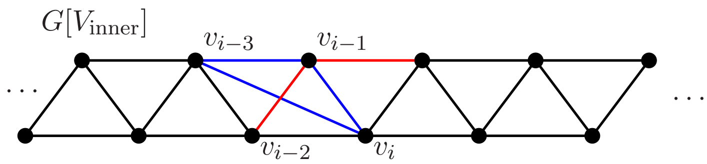

Figure 3.18: Colors determined by a reduced vertex v_{i-1}.

Consider the edge $v_{i-2}v_{i-3}$. Suppose this edge is colored blue. To avoid closing a blue cycle, the edge $v_{i-2}v_i$ must be red. Then to avoid a red cycle the edge v_iv_{i+1} must be blue. Continuing that way the colors of all edges to the right of the blue triangle in Figure 3.19 are uniquely determined. To the other side consider the parity of blue and red edges at v_{i-2}, this forces $v_{i-2}v_{i-4}$ to be blue, while the parity at v_{i-3} forces two red edges. To avoid a red cycle $v_{i-4}v_{i-5}$ must be blue, whence, parity forces $v_{i-4}v_{i-6}$ to be red. That way the color of edges left of the blue triangle is determined. The complete picture is shown in Figure 3.19: We have found a blue Z-structure.

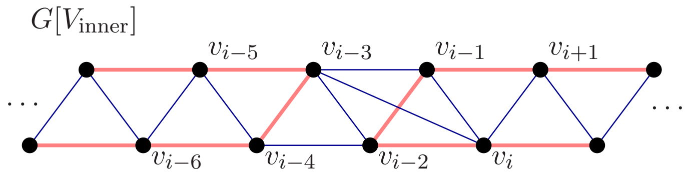

Figure 3.19: The blue edge $v_{i-3}v_{i-2}$ implies a blue Z.

Now suppose that the color of the edge v_{i-3}, v_{i-2} is red. Recalling that v_{i-1}, v_{i-2} and v_{i-1}, v_{i+1} are red consider the parity at v_{i-2} which forces v_{i-2}, v_i and v_{i-2}, v_{i-4} to be blue. Parity at v_i forces the red edges v_i, v_{i+1} and v_i, v_{i+2}. Hence, we have a red Z-structure in this case, see Figure 3.20.

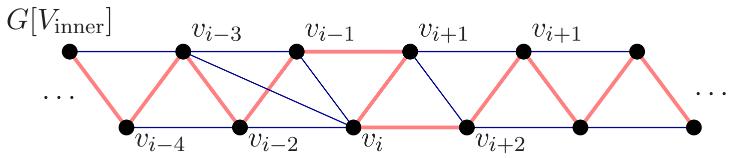

Figure 3.20: The red edge v_{i-3}, v_{i-2} implies a red Z.

We have seen that, given a modified vertex in $B_{n''}$, the parity condition and the cycle-freeness of the colored graphs induced by the inner vertices of $B_{n''}$ enforce a Z-structure. The zig-zag emanating from such a Z-structure in one direction has to run into the Z-structure of a second modified vertex. The outer paths of the other color make a turn at a modified vertex – and close a cycle at a second one. This is a contradiction since the blue triangles of the modified vertices are the only monochromatic cycles in $G[V''_{\text{inner}}]$. The contradiction shows that (for $n > 25000$) there is no 2-coloring of B_n, hence, the thickness of the graph is 3. $\square$

The above theorem disproves the conjecture of Dean et al. [8] that the class of bar 1-visibility graphs lies within the class of thickness-2 graphs. They showed that the reverse inclusion is not true by giving a (somewhat flawed) construction for a thickness-2 graph on n vertices which is not a bar 1-visibility graph, for all $n \geq 15$. Their technique is to construct two triangulations on the same vertex set but with disjoint edge sets, then the union of these two is a graph with $6n - 12$ edges which by Theorem 3.2 cannot be a B1V. We use their idea to strenghten the result:

Proposition 3.15. *There are thickness-*2 *graphs which are not bar* 1*-visibility graphs for all* $n \geq 9$.

Proof. Consider the two triangulations on nine vertices in Figure 3.21. Edges they have in common are emphasized; there are seven of them. Thus, the graph G on the same nine vertices with the union edge set has $2(3n-6)-7 = 6n-19$ edges. This graph obviously has thickness 2, but by Theorem 3.2 it is not a bar 1-visibility graph.

A graph with these properties on a larger vertex set can be constructed inductively from G: Choose a triangle in each of the plane layers such that the vertex sets of the two triangles are disjoint. Then add a new vertex with six neighbors, maintaining thickness 2: In both plane layers, place it into the chosen triangle and connect it to the three vertices of that triangle. Then the graph thus constructed has one additional vertex and six additional edges, therefore, it has still $6n - 19$ edges and is no B1V. □

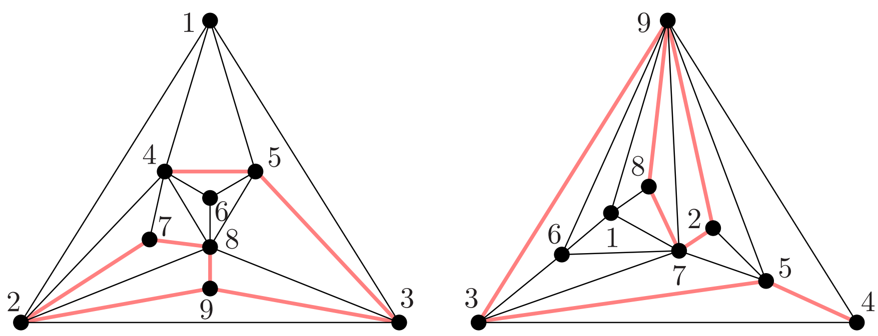

Figure 3.21: The union of these two triangulations has $6n - 12 - 7$ edges and therefore is no B1V.

Note that one cannot use the edge bound to find a graph on less than nine vertices which is not a B1V, since all graphs with on $n \leq 8$ vertices have no more than $6n - 20$ edges.

We have shown in this section that the class of bar 1-visibility graphs and the class of thickness-2 graphs are incomparable under inclusion. For bar 1-visibility graphs, the gap between the lower and upper bound is now as small as it can be (but still a gap): Are there B1Vs with thickness 4, or is 3 the correct upper bound? As in [19], we state the latter as conjecture:

Conjecture 1. *The thickness of bar* 1*-visibility graphs is at most* 3*.*

For general k, we have shown that there is a bar k-visibility of thickness $k+2$, unlike conjectured by Dean et al. in [8]. However, there is still a lot of space between this and the quadratic function shown in Theorem 3.11. Hereby the quadratic upper bound seems to be further away from the truth, as for $k = 1$ it yields 21 opposed to 3 or 4.

Chapter 4

Semi Bar *k*-Visibility Graphs

"One way to deal with this is to put everything into a big box
– which is a good way of dealing with many things in life."
Jiří Matoušek

This chapter introduces the class of semi bar k-visibility graphs (SBkVs). In the same way that bar k-visibility graphs are a generalization of bar visibility graphs, semi bar k-visibility graphs generalize semi bar visibility graphs (cf. Section 2). On the other hand, semi bar k-visibility graphs are a special case of bar k-visibility graphs. A good reason why this special case deserves extra treatment is the following: We will see that the strong combinatorial structure of SBkVs gives rise to a number of proof techniques yielding tight results for different graph parameters.

This chapter is organized as follows: In the first section, we get to know SBkVs by their definition and some simple observations. In Section 4.2 we use the latter to show a tight bound on the chromatic number of SBkVs. Then we will see an upper bound for the number of edges of our graphs in Section 4.3, and a corollary concerning their treewidth. Section 4.4 shows how to reconstruct a bar representation of an SBkV with maximum number of edges, in case some additional information is given. Section 4.5 is devoted to the connectivity of SBkVs. The main result of this chapter can be found in Section 4.6: We show that any SBkV has thickness at most 2 by presenting an algorithm which partitions the edges into two planar graphs.

4.1 Definition

Here we introduce semi bar k-visibility graphs and consider some simple properties in order to become familiar with these graphs. Recall that we defined *semi bars* to be bars extending from the y-axis to the right.

Definition 4.1. *A* semi bar k-visibility graph *(SBkV) is a bar k-visibility graph admitting a representation by x-different semi bars, i.e., a bar k-visibility representation in which all left endpoints of the bars are at $x = 0$, and the right endpoints have pairwise different x-coordinates.*

We always think of bar representations (which in this chapter is short for semi bar k-visibility representations) of SBkVs as rotated counterclockwise as in Figure 4.1, which shows an example of a semi bar 1-visibility graph and a corresponding bar representation.

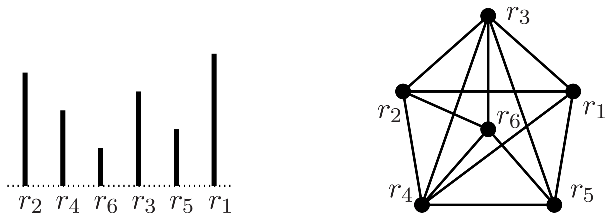

Figure 4.1: Example of a semi bar 1-visibility graph.

Let us make some more remarks analogous to those in the introduction to semi bar visibility graphs: The t-order lists bars from left to right, and the r-order by decreasing height. If the t-order is the canonical order of the natural numbers, then the permutation defined by the r-order uniquely defines the bar representation and thus the corresponding graph. For example, the B1VG in Figure. 4.1 is encoded by the permutation $(2, 4, 6, 3, 5, 1)$. Note that in the same way that a bar k-visibility representation induces a different (at least in general) BkV for every $k \geq 0$, the very same permutation encodes a different SBkV for every $k \geq 0$.

Where bar visibility graphs are planar, semi bar visibility graphs are even outerplanar – let us see in which way SBkVs behave better than BkVs. First it is easy to see (and will follow from the first theorem of this chapter) that SBkVs may very well be non-planar, for all $k > 0$; so at least they are not well-behaving enough to become entirely boring. But they have a useful property limiting their minimum degree and always providing a point of attack for induction proofs. Here is a definition of this property, taken from [32].

Definition 4.2. *A graph G is called ℓ-degenerate if every subgraph of G has a vertex of degree at most ℓ.*

Lemma 4.3. *Semi bar k-visibility graphs are ($2k + 2$)-degenerate for all $k \geq 0$.*

Proof. Let an SBkV G and a subgraph H of G be given, and consider a bar representation of G. Any bar has at most $2(k + 1)$ longer neighbors: Up to $k + 1$ to its left and up to $k + 1$ to its right. In particular, the vertex corresponding to the shortest bar in $B(V(H))$ has degree at most $2k + 2$ in H. □

One direction of the following proposition is an immediate corollary of this property.

Proposition 4.4. *K_{2k+3} is the largest complete SBkV, for all $k \geq 0$. Furthermore, an SBkV cannot contain a larger clique as a subgraph.*

Proof. Since SBkVs are $(2k+2)$-degenerate, no such graph can contain a complete subgraph on more than $2k+3$ vertices. – To see that K_{2k+3} is indeed an SBkV for any $k \geq 0$, consider Figure 4.2 which shows a schematic bar representation. □

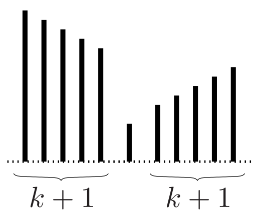

Figure 4.2: A complete SBkV on $2k+3$ bars.

Note that for any complete graph on $n \leq 2k+2$ vertices, a bar representation can be found by leaving out some of the bars in Figure 4.2.

Considering a bar in a bar representation of a given SBkV, it is often useful to distinguish between edges to longer bars and edges to shorter bars. For this reason, we often think of the edges as being directed from the vertex represented by the longer bar to the vertex represented by the shorter bar. Then we can speak of the *incoming edges* of a bar (which, of course, still is a slight abuse of notation), and of the *starting-bar* and *ending-bar* of an edge. Throughout this chapter, we will switch to this directed version of our graphs whenever it is useful.

4.2 Chromatic Number

Since we have seen that K_{2k+3} is an SBkV for every $k \geq 0$, we know that there are SBkVs with chromatic number $2k+3$. Now from the fact that SBkVs are $(2k+2)$-degenerate one can deduce that this trivial lower bound cannot be exceeded. The proof is mainly a standard argument showing that ℓ-degenerate graphs are $(\ell+1)$-colorable. However, we have to be a little careful since in general the property of being an SBkV is not closed under taking subgraphs.

Proposition 4.5. *The chromatic number of a semi bar k-visibility graph is at most $2k+3$, for all $k \geq 0$.*

Proof. We prove the assertion by induction on the number of vertices. If there are three or less vertices, the assumption is trivial. Now let G be an SBkV on $n > 3$ vertices, and let $\mathcal{B}$ be a bar representation of G. Consider the shortest bar and the corresponding vertex r_n, it has degree at most $2(k+1)$. By deleting $B(r_n)$ from $\mathcal{B}$, no new visibilities are created, and of course no old ones are blocked. Thus, the graph $G \setminus r_n$ is an SBkV and its vertices can be $(2k+3)$-colored by induction. Now r_n can be re-inserted and given a color not used by its neighbors. □

Together with the fact that complete SBkVs of size $2k+3$ exist, Proposition 4.5 implies that the largest possible chromatic number coincides with the size of the largest complete semi bar k-visibility graph. Graphs for which the chromatic number equals the clique number for every induced subgraph are called *perfect*. A necessary condition for a graph to be perfect is that it does not contain an induced C_{2k+1} for $k > 1$ (called *odd hole*), as these graphs have chromatic number 3 without containing a triangle. It is not much harder to see that a perfect graph cannot contain the complement of C_{2k+1} for $k > 1$ (an *odd antihole*) either. The celebrated Strong Perfect Graph Theorem [5] states that these necessary conditions are also sufficient: A graph is perfect if and only if it does not contain an odd hole or antihole. This beautiful characterization quickly settles the matter whether SBkVs belong to the class of perfect graphs. Figure 4.3 shows an example of a bar representation containing an induced C_5; thus, SBkVs in general are not perfect.

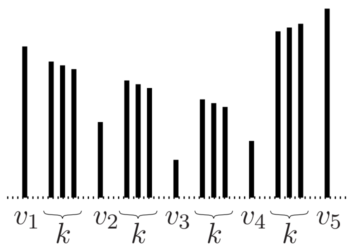

Figure 4.3: Example of a non-perfect SBkV: The v_i form an induced C_5.

4.3 Maximum Number of Edges

In this section, we show a tight upper bound for the maximum number of edges in an SBkV, and we look at the bar representations of SBkVs attaining this bound. Their structure can be described in a quite tangible way.

The last result of this section reveals a somewhat surprising consequence of this confined structure: Treewidth, a measure for the complexity of a graph, allows graphs to have a construction seemingly similar to our bar representations. But it turns out that from the structure of maximal SBkVs it follows that they can actually have large treewidth.

Let us start with some edge counting. If an SBkV on $n \leq 2k+3$ vertices is given, then by Proposition 4.4 the tight upper bound on its number of edges is $\binom{n}{2}$. For $n = 2k+2$ and $n = 2k+2$ this bound coincides with the bound for larger n given in the following theorem:

Theorem 4.6. *A semi bar k-visibility graph on $n \geq 2k+2$ vertices has at most $(k+1)(2n-2k-3)$ edges.*

Proof. Think of the edges as being directed from longer to shorter bars. Since each bar has at most $2(k+1)$ longer neighbors, each vertex has at most $2(k+1)$ incoming edges. Thus we have a first upper bound of $2n(k+1)$ on the number of edges.

Let us look more closely at the longest bars: The vertex r_1 corresponding to the longest bar does not have any incoming edges, r_2 has at most one, r_3 two, and so on until reaching r_{2k+2} which has no more than $2k+1$ incoming edges. Substracting these edges from the $2n(k+1)$ we obtain the desired upper bound:

$$2n(k+1) - \sum_{i=1}^{2k+2} i = 2n(k+1) - \frac{1}{2}(2k+2)(2k+3) = (k+1)(2n-2k-3)$$

□

We claim that this upper bound can be obtained. What could SBkVs with the maximum number of edges look like? The following conditions are necessary: The $2k+2$ longest bars have to induce a complete graph, and every shorter bar has to have $k+1$ incoming edges from either side. Now, a bar located at the boundary of the bar representation, corresponding to a vertex $v \in V_{\text{outer}} := \{t_1, t_2, \ldots, t_{k+1}\} \cup \{t_{n-k}, t_{n-k+1}, \ldots, t_n\}$, cannot have $k+1$ neighbors at either side. In consequence, V_{outer} has to be represented by the $2k+2$ longest bars.

Proposition 4.7. *For any $k \geq 0$ and $n \geq 2k+2$, there is a semi bar k-visibility graph with $(k+1)(2n-2k-3)$ edges.*

Proof. If a graph has a bar representation fulfilling the condition that the $2k+2$ longest bars constitute V_{outer} and form a complete graph, then all inner bars, respectively, all $v \in V \setminus V_{\text{outer}}$ have exactly $2k+2$ incoming edges. Now we can use the argumentation from the end of the previous proof – or calculate directly that the number of edges is

$$\begin{aligned}\binom{2k+2}{2} + (2k+2)(n-(2k+2)) &= (k+1)(2k+1+2n-4k-4) \\ &= (k+1)(2n-2k-3)\,.\end{aligned}$$

□

We call the graphs of the above proposition *maximal SBkVs*. All maximal SBkVs have a bar representation of the pattern shown in Figure 4.4. There is some more freedom in this pattern than the figure might suggest, as there are other orders in which the $2k + 2$ longest bars form a complete graph. We call these bars the *outer bars*, the remaining ones the *inner bars*. Corresponding to this, the vertices in $V_{\text{outer}} = \{t_1, t_2, \ldots, t_{k+1}\} \cup \{t_{n-k}, t_{n-k+1}, \ldots, t_n\}$ are denoted *outer vertices*, and the ones represented by inner bars are the *inner vertices*.

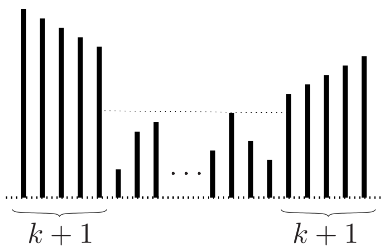

Figure 4.4: Structure of a maximal SBkV

Note that we can extend every SBkV to a maximal one, i.e., every SBkV is a subgraph of a maximal SBkV: Prolongate the outer bars $B(t_1)$ and $B(t_n)$ until they are the longest ones. This can always be done, since it can only introduce new lines of sight. Then add k longer bars left and k longer bars right of the bar representation, such that they form a complete K_{2k+2} together with t_1 and t_n. The graph induced by this bar representation clearly is a maximal SBkV.

We now seem to have a quite good idea of the structure of maximal SBkVs: We can build all of them by starting with $2k + 2$ bars inducing a clique and inserting bars in the middle one by one, by order of their length. Each inserted bar then is adjacent to $2k + 2$ longer neighbors. There is a graph parameter measuring how far a graph is from being a tree which allows a similar inductive construction. Let us take a little detour to graph treewidth.

Definition 4.8. *For a vertex v and a set of vertices S we say that v is* universal *to S if v is adjacent to all the vertices in S.*
*A graph G is an ℓ-*tree *if it is either a K_ℓ or it is formed from an ℓ-tree G' by adding a new vertex that is universal to a K_ℓ in G'.*
A graph has treewidth *at most ℓ if it is a subgraph of an ℓ-tree.*

The above definition is taken from [7]. (Note that the literature usually speaks of k-trees, but we use a different parameter here since k is already busy.) Rose [28] proved several equivalent characterizations of ℓ-trees, one of them will be especially useful for us:

Lemma 4.9. *A graph G on n vertices is an ℓ-tree iff G is connected, has exactly $\ell n - \frac{1}{2}\ell(\ell + 1)$ edges, and every minimal separator of G is a k-clique.*

Now we see how the inductive construction of $(2k + 2)$-trees as described in Definition 4.8 ressembles our construction of maximal SBkVs: There too we start with a clique and insert vertices adjacent to $2k + 2$ neighbors in the already constructed part. In the case of SBkVs, these neighbors might not be pairwise adjacent – but still, it is tempting to think that SBkVs have treewidth at most $2k+2$. The following proposition shows that this is misleading.

Proposition 4.10. *For each $k > 0$, there is a semi bar k-visibility graph with treewidth larger than $2k + 2$.*

Proof. From Lemma 4.9 we know that an ℓ-tree on n vertices has $\ell n - \frac{1}{2}l(l + 1)$ edges, and for $\ell = 2k + 2$, this is exactly $(k + 1)(2n - 2k - 3)$. Now, if a maximal SBkV G has treewidth at most $2k + 2$, it must be a subgraph of a $2k + 2$-tree, and since they have the same number of edges, G must be a $2k + 2$-tree itself! Thus, we can find a vertex order such that the first $2k + 2$ vertices form a K_{2k+2}, and all other vertices are universal to $2k + 2$ preceding vertices which form a complete graph.

Consider the maximal SBkV G on $2(k + 1) + 3$ vertices represented in Figure 4.5. For the sake of contradiction assume that it is a $(2k + 2)$-tree. Then from the definition of $(2k+2)$-tree it follows that any vertex of G is part of a $(2k+3)$-clique. Now consider the vertex t_{k+4}. It has only $2k+2$ neighbors in G, thus they need to be pairwise adjacent to form a $(2k + 3)$-clique containing t_{k+4}. But for $k > 0$, the neighborhood of t_{k+4} is not complete, since t_{k+3} blocks the sight between t_{k+2} and t_n. This is the desired contradiction. Thus G is not a $(2k + 2)$-tree, and with the above it follows that it has treewidth larger than $2k + 2$. □

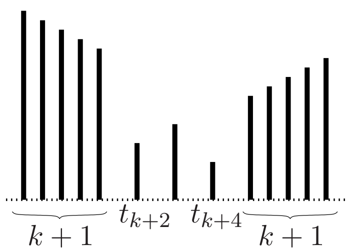

Figure 4.5: An SBkV with treewidth larger than $2k + 2$

For $k = 0$, maximal SBkVs are just maximal outerplanar graphs. From their triangulated structure it is easy to see that they can be constructed from a K_2 by successively adding a vertex adjacent to two vertices already connected by an edge. Thus, all maximal outerplanar graphs are 2-trees, and any semi bar visibility graph has treewidth at most 2.

In Section 4.5 we will investigate another connection between SBkVs and ℓ-trees. Before, we want to gain further insight into the structure of maximal SBkVs in the next section.

4.4 Reconstructing Semi Bar *k*-Visibility Representations

One of the first questions one might ask about semi bar k-visibility graph is how to find a bar representation of a given graph which is known to be an SBkV. For maximal SBkVs this can nicely be done using their $(2k+2)$-degenerateness, as we show in this section. However, we have to give some additional information as input.

Proposition 4.11. *For $k \geq 0$, let a maximal SBkV G be given with a fixed t-order of its vertices. Then an r-orders of the vertices can be computed which, together with the given t-order, defines a bar representation inducing G.*

Proof. Since G is maximal, we know that the first and the outer vertices in the given t-order correspond to the $2k+2$ longest bars. Now the idea is to choose one of the inner vertices (if there are) which will correspond to the shortest bar of the representation we are constructing. Then we delete this vertex from G. This can be iterated until all inner vertices have been chosen. By adding a suitable order of the outer vertices we obtain a complete order of V which is the reverse of an r-order inducing G.

Let us look at the process in more detail. By Lemma 4.3 we know that any induced subgraph of G contains a vertex of degree at most $2k+2$. For example, the shortest bar of a bar representation of G represents such a vertex. From the structure of maximal SBkVs it follows that in fact there is no vertex of smaller degree (cf. Figure 4.4). Thus in any step, we can choose a vertex of degree $2k+2$ and delete it. Let v_i, $i = 1, 2, \ldots, n-2k-2$, be the order of the deleted vertices, and let G_i denote the graph obtained after deleting $v_1, \ldots, v_i$, with $G_0 = G$. Then by the choice of v_i, its degree in G_{i-1} is exactly $2k+2$, for any $i = 1, \ldots n-2k-2$. We claim that G_{i-1} has a bar representation in which v_i corresponds to the shortest bar.

The claim is automatically fulfilled for $i = n-2k-2$, since apart from v_i only outer vertices are left in G_{i-1} in this case. Now let $i < 2k-2$, let $\mathcal{B}$ be a bar representation of G_{i-1}, and suppose that $B(v_i)$ is not the shortest bar of this representation. Assume that $v_i = t_p$ with $p \in \{k+2, \ldots, n-2k-2\}$. Note that $B(t_p)$ sees all $B(t_q)$ in its *trivial neighborhood*, that is, all $B(t_q)$ with $p-k-1 \leq q \leq p+k+1$ and $q \neq p$. Thus these bars correspond exactly to the $2k+2$ neighbors of $t_p = v_i$ in G_{i-1}. (Figure 4.6 shows an example for the case $k = 1$; here, the two bars left and the two bars right of each bar form its trivial neighborhood.) If any bar of the trivial neighborhood is shorter than $B(t_p)$, then $B(t_p)$ can see beyond this bar, and there is an additional line of sight to a bar outside of the trivial neighborhood. This results in more than $2k+2$ edges incident to $t_p = v_i$, which is a contradiction to the choice of v_i. Thus, all bars in the trivial neighborhood of $B(t_p)$ are longer than $B(t_p)$. Now shortening $B(t_p)$ until it is the shortest bar in $\mathcal{B}$ does not block any lines of sight, nor can it introduce new ones, as no line of sight can traverse the $k+1$ bars on either side of $B(t_p)$. Hence $B(v_i)$ can be chosen to be the shortest bar in a bar representation of G_{i-1}, as claimed.

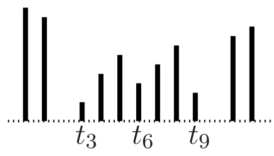

Figure 4.6: A bar representation of a maximal SB1V G. Possible choices for the shortest bar in a bar representation of G apart from t_3 are t_6 and t_9: Each of them has degree 4.

Now we set $r_n = v_1$, $r_{n-1} = v_2$, ..., $r_{2k+3} = v_{n-2k-2}$. For the $2k+2$ outer bars, we choose any order which yields a complete graph; for example $r_1 = t_1$, ..., $r_{k+1} = t_{k+1}$, $r_{k+2} = t_n$, ..., $r_{2k+2} = t_{n-k}$ (cf. Figure 4.4). Then the resulting r-order yields a semi bar k-visibility representation of G: If $B(r_p)$ is not among the $2k+2$ longest bars, then the $2k+2$ longer neighbors of $B(r_p)$ correspond exactly to the $2k+2$ neighbors of $r_p = v_i$ in G_{i-1}. (Note that we have $i = n-p+1$.) On the other hand, any edge of G that is not already contained in the $(2k+2)$-clique of the outer vertices is incident to a v_i and thus realized in the constructed bar representation. We conclude that any r-order constructed as above yields a bar representation of G with the prescribed t-order of the vertices. □

The above construction does not just yield one r-order inducing G with the given t-order, one can in fact find *all* such bar representations of G this way: Any fixed bar representation of G defines an r-order of the vertices in which the first $2k+2$ vertices form a clique, and in which each vertex has only $2k+2$ neighbors with larger r-index. By definition of the construction any such order can be found as described above.

4.5 Connectivity

In this section, we want to determine the connectivity of a bar k-visibility graph $G = (V, E)$ given with bar representation $\mathcal{B}$. It is clear that G is connected, and it is not too hard to guess that its connectivity is $k+1$. To prove this, we first have a look at the structure of a special subgraph of G: There are some edges that are always contained in E, independently of the permutation encoding G. These *trivial edges* provide another connection between SBkVs and ℓ-trees.

Definition 4.12. *Let an SBkV $G = (V, E)$ with bar representation $\mathcal{B}$ be given. Let $V = \{t_1, t_2, \ldots, t_n\}$ in the t-order induced by $\mathcal{B}$. An edge $t_it_j \in E$ is called a* trivial edge *if $|i - j| \leq k + 1$.*

Lemma 4.13. *The trivial edges of a semi bar k-visibility graph on at least $k + 1$ vertices form a $(k + 1)$-tree.*

Proof. Consider a bar representation of an SBkV G. The crucial observation is that any set of up to $k + 2$ successive bars in the t-order represents a complete graph. In particular this holds for the leftmost $k + 1$ bars. Now assume inductively that the graph induced by $B(t_1), B(t_2), \ldots, B(t_i)$, with $i > k + 1$, is a $(k + 1)$-tree. The next bar, $B(t_{i+1})$, forms a complete graph with its $k + 1$ trivial neighbors $B(t_{i-k}), B(t_{i-k+1}), \ldots, B(t_i)$. It is easy to see that these are its only trivial neighbors in $G[t_1, t_2 \ldots, t_i]$. Thus, t_{i+1} is universal to a K_{k+1} in G, and the trivial edges form a $(k + 1)$-tree. □

Theorem 4.14. *Semi bar k-visibility graphs on more than $k+1$ vertices are $(k+1)$-connected.*

Proof. From the previous lemma we know that each SBkV on enough vertices contains a $(k + 1)$-tree spanning all of its vertices. Now by the characterization of Lemma 4.9, $(k + 1)$-trees are $(k + 1)$-connected. Thus, any SBkV as in the statement contains a $(k+1)$-connected spanning subgraph and is therefore $(k+1)$-connected. □

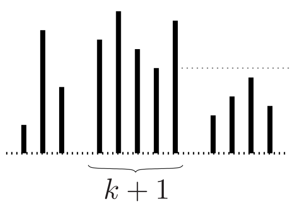

Figure 4.7: A bar representation containing a $(k + 1)$-separator

Figure 4.7 shows that in general an SBkV can have a $(k + 1)$-separator. If we delete the $k + 1$ vertices corresponding to the bars in the middle, the graph falls apart into the two components induced by the three bars on the left and the remaining ones on the right side. There is an explicit way of characterizing the $(k + 1)$-separators:

Proposition 4.15. *Let $G = (V, E)$ be an SBkV given with a bar representation $\mathcal{B}$ and a corresponding t-order of V. Let $S \subset V$. Then S is a $(k+1)$-separator of G if and only if $S = \{t_i, t_{i+1}, \ldots, t_{i+k}\}$ for some i with $1 < i < n-k$, and left or right of $B(S)$ in $\mathcal{B}$ all bars are shorter than the shortest one in $B(S)$.*

Proof. We first show that the two conditions are necessary for S to be a $(k+1)$-separator. In order to separate the $(k+1)$-tree built by the trivial edges of G, the vertices of S have to be successive in the t-order, without being located at one of its ends. This proves the first condition. Now let $S = \{t_i, t_{i+1}, \ldots, t_{i+k}\}$ with $1 < i < n-k$. Let $B(t_j)$ be the shortest bar in $B(S)$. Suppose that left and right of $B(S)$ there is a bar longer than $B(t_j)$. Let $B(t_\ell)$ be the rightmost such bar left of $B(S)$, and let $B(t_m)$ be the leftmost such bar right of $B(S)$. Then there is a line of sight between $B(t_\ell)$ and $B(t_m)$, since there are at most k longer bars which could cloud it. The edge $t_\ell t_m$ connects the two paths $t_1, \ldots, t_{i-1}$ and $t_{i+k+1}, \ldots, t_n$. Thus, S cannot be a separating set.

For the reverse direction observe that any set of vertices with the described two properties separates the vertices corresponding to the “shorter half” of the bar representation from the rest of the graph (see Figure 4.7), and thus is a $(k+1)$-separator. □

Using the characterization of Proposition 4.15 one can efficiently find all the $(k+1)$-separators of an SBkV which is given by a permutation defining a bar representation. This is done by running through the vertices following the t-order, retaining the longest already seen and the longest not yet seen bar, and checking for each set of $k+1$ successive bars if the shortest among them is longer than one of the two retained ones.

Another observation follows from the above proposition: If $S_i = \{t_i, \ldots, t_{i+k}\}$ and $S_j = \{t_j, \ldots, t_{j+k}\}$ with $j > i$ are $(k+1)$-separators of G successive in the t-order, i.e., there is no $(k+1)$-separator $S_\ell = \{t_\ell, \ldots, t_{l+1}\}$ with $i < l < j$, then the graph induced by the bars $t_i, t_{i+1}, \ldots, t_{j+k}$ is ($k+2$)-connected.

One might already suspect by now that the connectivity of maximal SBkVs is higher than those of ordinary SBkVs. This can be made precise by further exploring the structure of their bar representations. We will use the global version of Menger’s Theorem (see e.g. [12]) which states that a graph is ℓ-connected if and only if it contains ℓ independent paths between any two vertices.

Proposition 4.16. *Maximal semi bar k-visibility graphs on more than $2k+2$ vertices are ($2k+2$)-connected.*

Proof. Let $G = (V, E)$ be a maximal SBkV with $|V| > 2k+2$. We will show that there are $2k+2$ vertex-disjoint paths between any two vertices $t_i, t_j \in V$ with $i > j$, then with Menger’s Theorem it follows that G is ($2k+2$)-connected. The idea is to define packages of $k+1$ vertices and find bundles of $2(k+1)$ paths using them.

Let us first assume that $j > i + k$. Let $P_r(t_i) := \{t_i, t_{i+1}, \ldots, t_{i+k}\} \subset N(t_i)$ and $P_\ell(t_j) := \{t_{j-k}, t_{j-k+1}, \ldots, t_j\} \subset N(t_j)$. Note that $j \notin P_r(t_i)$ and $i \notin P_\ell(t_j)$. Now we start at some bar in $B(P_r(t_i))$ and build a *jumping path* by successively jumping $k+1$ bars to the right until we end up in $B(P_\ell(t_j))$. See Figure 4.8 for illustration.

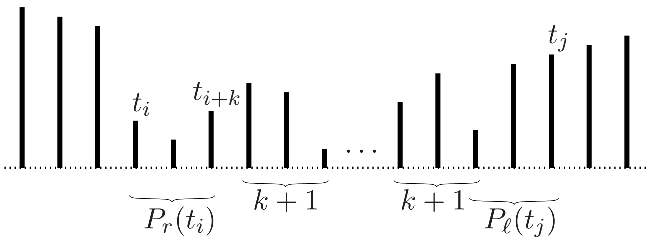

Figure 4.8: The bars between $B(t_i)$ and $B(t_j)$ form $k+1$ disjoint *inward paths*.

We can find $k+1$ disjoint t_i-t_j-paths by adding (where needed) the edge between t_i and the start-vertex of the jumping path, as well as the one between its end-vertex and t_j. If there are exactly k bars between $B(t_i)$ and $B(t_j)$, the edge t_it_j exists and constitutes one of the paths. Let us call the paths defined in this way the *inward paths* as they only use vertices which are between t_i and t_j in the t-order.

Now we will use a similar construction to find $k+1$ disjoint *outward paths*: Let $L := \{t_1, t_2, \ldots, t_{k+1}\}$ be the package of the left outer vertices, and let $R := \{t_{n-k}, \ldots, t_n\}$ consist of the right ones. If $t_i \in L$, set $P_\ell(t_i) := L$, otherwise define $P_\ell(t_i) := \{t_{i-k}, t_{i-k+1}, \ldots, t_i\}$. Similarly, let $P_r(t_j) := R$ if $t_j \in R$, and define $P_r(t_j) := \{t_j, t_{j+1}, \ldots, t_{j+k}\}$ otherwise. Now for any $v \in P_\ell(t_i)$ build a (possibly trivial) jumping path starting in v and ending in L. On the other side, build paths connecting $P_r(t_j)$ and R. We know that $L \cup R$ forms a complete graph. Use any matching between the vertices in L and those in R to obtain $k+1$ disjoint paths between t_i and t_j.

Now we still have to consider the case where $j = i + \ell$ with $1 \leq \ell \leq k$, note that then we have $t_it_j \in E$. In this case not enough bars between $B(t_i)$ and $B(t_j)$ exist to find $k+1$ disjoint paths using only those, therefore we extend the allowed range for inward paths. With this trick we will find $2k+2-\ell$ disjoint inward paths and ℓ disjoint outward paths between t_i and t_j (see Figure 4.9).

If t_i and t_j both belong to L or both to R, they are part of the same $(2k+2)$-clique. Thus, we get $2k+1$ disjoint paths between them for free, and the last one can easily be constructed from a jumping path using the inner bars. Therefore we can assume that $j > k+1$ and $i < n-k-1$.

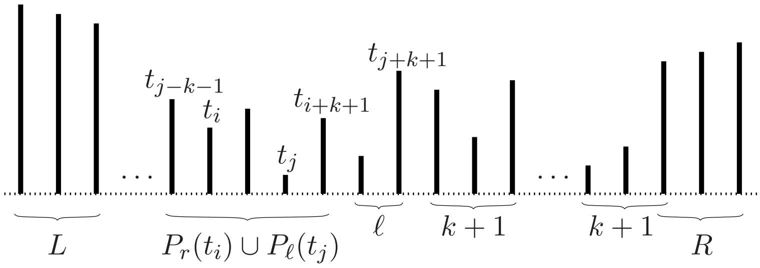

Figure 4.9: If $j = i + \ell$ with $\ell \leq k$, we find $2k + 2 - \ell$ paths in $P_r(t_i) \cup P_\ell(t_j)$, and ℓ outward paths.

Let us consider the set $P_r(t_i) \cup P_\ell(t_j) = \{t_{j-k-1}, t_{j-k}, \ldots, t_{i+k+1}\}$, these are the vertices which are trivial neighbors of both t_i and t_j. With $j = i + l$ it follows that there are $i + k + 1 - (j - k - 2) = 2k + 3 + i - j = 2k + 3 - l$ of them, among them t_i and t_j. Thus we find $2k + 2 - l$ disjoint $(t_i - t_j)$-paths; one of them is the edge t_it_j, the others all consist of exactly two edges. To find ℓ outward paths we use jumping paths and a matching between the boundary vertices as in the first case, this time starting with $P_\ell(t_i) = \{t_{i-k-1}, t_{i-k}, \ldots, t_{j-k-2}\}$ and $P_r(t_j) = \{t_{i+k+2}, \ldots, t_{j+k+1}\}$. In this way we find $j + k + 1 - (i + k + 1) = j - i = l$ outward paths which are pairwise disjoint and also disjoint from the inward paths defined before. □

Note that it is clear that the connectivity of an arbitrary SBkV cannot be larger than $2k + 2$, since the shortest bar has at most that many neighbors.

4.6 Thickness of Semi Bar 1-Visibility Graphs

Here we come to the results that inspired the introduction of semi bar k-visibility graphs. Let us again consider the special case $k = 1$. Whereas the thickness of general B1Vs can exceed the previously conjectured bound of 2 (cf. Section 3.8), semi bar 1-visibility graphs can indeed always be partitioned into two planar graphs, as we will see in this section.

Between the full class of B1Vs and the subclass containing all SB1Vs there is the class of bar 1-visibility graphs admitting a representation by a set of bars such that there is a vertical line stabbing all bars of the representation. Note that the proof of Section 3.8 implies that already in this intermediate class there are graphs of thickness 3.

Now let $G = (V, E)$ be an SB1V given by a bar representation. In this section we present an algorithm which 2-colors the edges of G such that each color class forms a plane graph in an embedding induced by the bar representation. Consequently the thickness of any SB1V is at most 2.

4.6.1 1-Bend Drawing

As helpful tool for the following we introduce a drawing of semi bar 1-visibility graphs in the plane in which each edge is a polyline with at most one bend, called a 1-bend drawing. This drawing is not planar in general, but it will assist us with constructing and analyzing the edge partition. The best explanation of the 1-bend drawing is probably Figure 4.10.

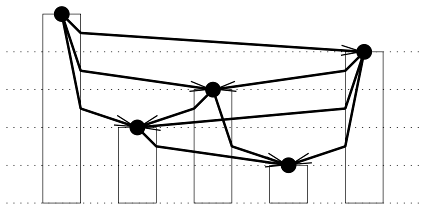

Figure 4.10: The 1-bend drawing of an SB1V

Here is a more formal definition of the drawing: Enlarge the bars of each vertex v to a rectangle $B(v)$ with a uniform width. Recall that we assume that the heights of all bars are different and that $B(r_1)$, $B(r_2), \dots, B(r_n)$ lists the bars by decreasing height. Assign the *stripe* between the horizontal line touching the top of bar $B(r_i)$ and the horizontal line touching the top of bar $B(r_{i-1})$ to $B(r_i)$. The dotted lines in Figure 4.10 separate the stripes. Embed each vertex v at the midpoint of the upper boundary of $B(v)$. We think of the edges as being directed from the longer bar (its *starting bar*) to the shorter bar (its *ending bar*).

Now draw each edge $e = r_i r_j$ composed of two segments; the first segment is contained in $B(r_i)$, it connects r_i with the inflection point x_e, the second segment connects x_e with r_j within the stripe of r_j. A good choice which bewares from crossings between edges emanating from r_i is to place x_e on the vertical boundary of $B(r_i)$ which is closer to r_j, with a height which is inside the stripe of r_j. We call the segment (r_i, x_e) the *vertical part*, the segment (x_e, r_j) the *horizontal part* of the edge. Note that the stripe associated with $B(v)$ contains the horizontal parts of the incoming edges of v. Other edges might cross this stripe, but only with their vertical parts.

4.6.2 2-Coloring Algorithm

Let an SB1V be given with a 1-bend drawing as described above. We now present the algorithm 2PLANAR providing a partition of the edges into two planar graphs (both on the vertex set V), using the given embedding. Thus, the algorithm produces planar embeddings of the two graphs such that each edge has at most one bend. We think of the partition of the edges as a 2-coloring with colors blue and red. The idea of the algorithm is the following: Given the 1-bend drawing, start with r_1, color all outgoing edges, move on to r_2, and so on. The algorithm uses an auxiliary coloring of the bars to determine the color of the edges.

Algorithm 2PLANAR

1. Start with r_1. Color $B(r_1)$ and all outgoing edges of r_1 blue. Whenever such an edge traverses another bar, color that bar red.
2. For $i = 2, \ldots, n-1$
   If $B(r_i)$ is uncolored, then color this bar blue.
   For each uncolored edge $e = r_i r_j$
   (a) If e is a direct edge, it obtains the color of its starting bar $B(r_i)$.
   (b) If e is an indirect edge, check if the traversed bar has a color. If so, e obtains the other color. Otherwise, it receives the color of its starting bar $B(r_i)$, and the traversed bar gets the opposite color.

Note that 2PLANAR defines a unique color for every edge. Figure 4.11 illustrates the result.

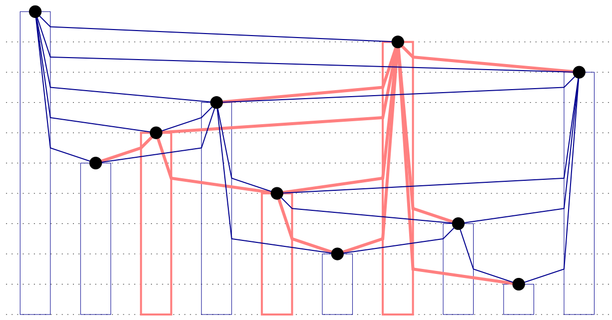

Figure 4.11: A coloring produced by the algorithm.

We observe that 2(b) implies the following:

Invariant. Whenever an edge traverses a bar, the colors of the edge and the traversed bar are different.

The following lemma will help showing the correctness of the algorithm:

Lemma 4.17. *If $B(v)$ is an arbitrary bar, then at most one longer bar can be the starting bar of indirect edges traversing $B(v)$.*

Proof. Assume that $x = x_1x_2$ is an edge traversing $B(v)$ with $B(x_1)$ longer than $B(v)$, such that $B(x_2)$ is the shortest ending bar among all such edges. Then we know that between $B(x_1)$ and $B(v)$ in the t-order there can be no bar longer than $B(x_2)$, else it would block the line of sight corresponding to x, see Figure 4.12.

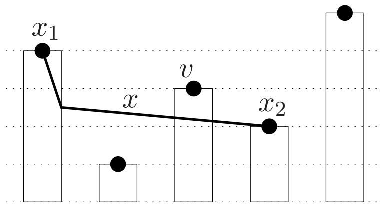

Figure 4.12: Only one longer bar can send edges through B(v).

Suppose there is another edge $y = y_1y_2$ starting from a bar $B(y_1)$ which is longer than $B(v)$. As y can traverse only one bar it must connect to a bar $B(y_i)$ which is between $B(v)$ and $B(x_1)$ in the t-order. Moreover, the choice of x implies that the horizontal part of y lies above the horizontal part of x. But then the bar $B(y_i)$ has to be longer than $B(x_2)$! This contradicts the conclusion of the previous paragraph. □

Proposition 4.18. *2PLANAR produces a partition of E into two plane edge sets.*

Proof. We have to show that in the 2-coloring computed by 2PLANAR, any two crossing edges have different colors.

The vertical part of every edge runs within its starting-bar, and the only vertical parts occuring inside of each bar are parts of edges that start at the corresponding vertex. Thus, vertical parts of edges do not cross.

The horizontal part of every edge runs within one stripe, and the only horizontal parts occuring inside of each stripe are parts of edges ending at the associated vertex. Thus, horizontal parts of edges do not cross.

Consider two crossing edges e and f. From the above we infer that the crossing appears between the vertical part of one edge (say, e) and the horizontal part of another edge (say, f). Hence, the crossing point takes place inside of the starting-bar of e, and the edge f is an indirect edge traversing this bar (see Figure 4.13).

Let the start-vertex of e be e_1 and its end-vertex e_2. Similarly, let f lead from f_1 to f_2. Suppose that the color of f is red, then the invariant implies that $B(e_1)$ is blue.

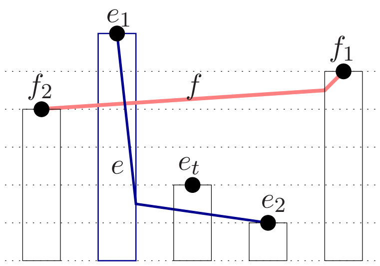

Figure 4.13: Two crossing edges. There can be many shorter bars between those depicted here, as long as they do not block the lines of sight representing e and f.

If e is a direct edge it obtains the color of its starting bar, in this case blue. Thus, assume that e is an indirect edge. Then its color depends on the color of the traversed bar, let $B(e_t)$ be this bar. (Note that $e_t = f_1$ or $e_t = f_2$ are possible.)

First let us assume that $B(e_t)$ is shorter than $B(e_1)$. Then by Lemma 4.17 we know that $B(e_1)$ is the only longer bar sending an edge (e.g. the edge e) through $B(e_t)$. Therefore $B(e_t)$ was still uncolored when the algorithm considered $B(e_1)$, and thus e is colored with the color of $B(e_1)$, which is blue. This shows that the edges e and f have different colors in this case.

If $B(e_t)$ is longer than $B(e_1)$, then we can deduce $e_t = f_1$. For if a bar longer than $B(e_t)$ would be located strictly between $B(f_1)$ and $B(f_2)$ in the t-order, the line of sight corresponding to f would have to traverse two bars ($B(e_1)$ and this longer bar), which is a contradiction. In addition, we know that $B(f_2)$ is shorter than $B(e_1)$, else e and f would not cross. Thus, we have $e_t = f_1$, and $B(f_1)$ is longer than $B(e_1)$. Since f traverses $B(e_1)$, the Lemma 4.17 tells us that $B(f_1)$ is the only longer bar sending an edge through $B(e_1)$. It follows that $B(e_1)$ was still uncolored when algorithm considered $B(f_1)$. Therefore, the red color of f was chosen equal to the color of the bar $B(f_1)$. Our invariant now implies that the edge e, traversing the red bar $B(f_1)$, is blue. Hence, again e and f have different colors and we have shown that both edge classes are plane. □

Now we haven proven the second main result of this diploma thesis:

Theorem 4.19. *Semi bar* 1*-visibility graphs have thickness at most* 2*.*

The algorithm shows that SB1Vs have *graph-theoretic* thickness at most 2, and it provides a partition of the edges into two planar graphs, providing two plane embeddings. But as the edges are not straight lines, this does not show that the *geometric thickness* is bounded by 2. This variation of thickness is defined as follows:

Definition 4.20. *The geometric thickness of a graph G is the smallest value of k such that we can assign planar point locations to the vertices of G, represent edges of G as straight line segments, and assign each edge to one of k layers such that no two edges in the same layer cross.*

Geometric thickness was first introduced by Dillencourt, Eppstein and Hirschberg in [13]. In [15], Eppstein showed that graph-theoretic thickness and geometric thickness are not even asymptotically equivalent. Still, we think that any SB1V has a straight-line embedding such that the edges can be partitioned into two plane graphs. Maybe one can even use 2PLANAR to partition the edges – it remains to find a clever way of removing the bends from the 1-bend drawing. For emphasis let us state this as conjecture.

Conjecture 2. *Semi bar* 1*-visibility graphs have geometric thickness at most* 2*.*

4.6.3 Structure of the Blue and Red Graph

Given a semi bar 1-visibility graph $G = (V, E)$, we can say more about the effect of the algorithm 2PLANAR on G: It partitions the edges evenly among the blue and the red graph. As *blue graph* let us define $G_{\text{blue}} := (V', E_{\text{blue}})$ by taking all blue edges on the vertex set V and deleting isolated vertices. The *red graph* is defined analogously as $G_{\text{red}} := (V'', E_{\text{red}})$. Recall that from Theorem 4.6 we know that an SB1V has at most $(k+1)(2n-2k-3) = 4n-10$ edges.

Proposition 4.21. *The blue and the red graph each contain at most* $2n-3$ *edges.*

Proof. We count the incoming blue edges at each vertex and claim that there are at most two of them. See Figure 4.14 for an illustration. Consider a bar $B(v)$ and the closest bar to the left (say) of it that is the starting bar $B(w)$ of an incoming blue edge at v. Either such an edge springs from a direct line of sight between $B(v)$ and the blue bar $B(w)$, or it is induced by an indirect line of sight traversing a red bar $B(u)$.

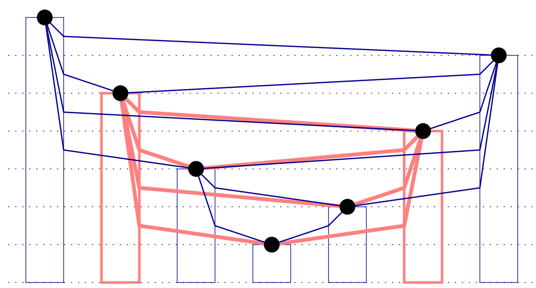

Figure 4.14: Example of an SB1V with $2n-3$ blue edges.

In the first case, any other incoming blue edge from the left has to traverse $B(w)$ and therefore is colored red. In the second case, any other such edge would have to traverse $B(w)$ as well as $B(u)$, which is not possible.

Thus there is at most one incoming blue edge from each side, which yields an upper bound of $2n$ blue edges. But the vertex r_1 represented by the longest bar has no incoming edges, and r_2 has only one. Therefore we can substract three edges, obtaining the desired result. The same argument applies to the number of red edges. □

Note that the only properties of 2PLANAR that we used in this proof are our invariant (any edge traversing a bar has the opposite color of the bar it traverses) and the fact that any direct edge earns the color of its starting-bar. We will need this in the following section.

The upper bound of Proposition 4.21 is sharp, as the blue graph in Figure 4.14 shows: Any vertex except for r_1 and r_2 has two incoming edges. The pattern shown by the example in the figure can be used to construct an SB1V with $2n - 3$ blue edges for arbitrary n.

The edge bound of $2n - 3$ may sound familiar – it also holds for outerplanar graphs. However, the example in the figure shows that, in general, G_{blue} and G_{red} are not outerplanar: The blue graph induced by the five longest bars forms a $K_{2,3}$. In Figure 4.15, the red graph induced by the vertices t_2, t_3, t_5, t_6 and t_7 contains K_4 as a minor, which can be obtained by contracting the edge t_3t_5.

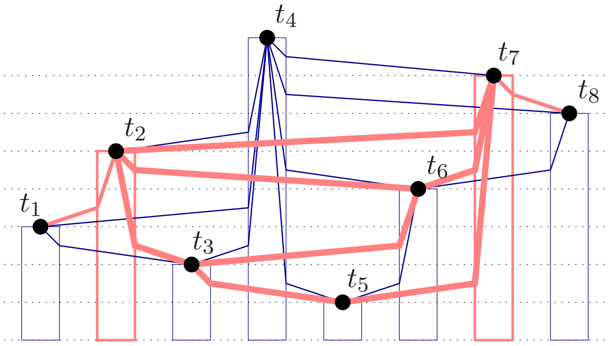

Figure 4.15: The red graph contains K_4 as a minor.

4.6.4 Maximal Blue and Red Graphs

Proposition 4.21 hints that there might be more structure to explore within the blue and the red graph defined by 2PLANAR. This turns out to be especially fruitful when examining maximal SB1Vs, as we will see in this section: In this case, G_{blue}

and G_{red} belong to the class of *Laman graphs*. We will define this in detail below, first let us specify the graphs we are talking about.

For the rest of this section, let G be a maximal SB1V on n vertices given with a bar representation $\mathcal{B}$. Let its edges be colored by 2PLANAR and define G_{blue} and G_{red} as in the previous section. Suppose without restriction that $t_1 = r_1$ and $t_n = r_2$. From the structure of maximal SB1Vs (cf. Section 4.3) we also know that $\{t_2, t_{n-1}\} = \{r_3, r_4\}$. We observe that 2PLANAR colors $B(r_1)$ and $B(r_2)$ blue, and the two corresponding vertices only have blue incident edges, see Figure 4.14. Note that this implies that $V(G_{\text{red}})$ does not contain t_1 and t_n. The following is a corollary of Proposition 4.21 and shows that in our setting, $V(G_{\text{blue}}) = V(G)$ and $V(G_{\text{red}}) = V(G) \setminus \{t_1, t_2\}$:

Lemma 4.22. *G_{blue} has exactly $2n-3$ and G_{red} exactly $2n-7$ edges.*

Proof. From Proposition 4.21 we know that G has at most $2n-3$ blue and red edges, respectively. We can also apply this proposition to G_{red} to see that it has at most $2(n-2)-3 = 2n-7$ edges. Since G has exactly $4n-10$ edges by Proposition 4.7 it follows that G_{blue} has exactly $2n-3$ and G_{red} exactly $2n-7$ edges. □

Now let us look at the definition of Laman graphs and see why maximal red and blue graphs fulfill it.

Definition 4.23. *A graph $G = (V, E)$ is called a* Laman graph *if $|E| = 2|V| - 3$ and $|E[V']| \leq 2|V'| - 3$ for all $V' \subset V$ containing at least two vertices.*

Theorem 4.24. *G_{blue} and G_{red} of a maximal SB1V G are Laman graphs.*

Proof. We show the assertion for $G_{\text{blue}} =: (V, E)$, the red case can be proven analogously. As G is a maximal SB1V, we know from Lemma 4.22 that $|E| = 2|V| - 3$. It remains to show that $|E[V']| \leq 2|V'| - 3$ for all $V' \subset V$ with $|V'| \geq 2$. Consider such a set V' and the set of bars $B(V')$ representing V' in the given bar representation $\mathcal{B}$ of G. The coloring of $E[V']$ and $B(V')$ induced by the given coloring of G still fulfills the invariant of 2PLANAR and has the property that every direct edge has the color of its starting-bar. Therefore, an argument analogous to the proof of Proposition 4.21 shows that $E[V']$ contains at most $2|V'| - 3$ edges. □

Several equivalent characterizations of Laman graphs are known; we will state one in the theorem below. The proof and more about Laman graphs, especially about their significance for rigidity of graphs in the plane, as well as references to the original proofs, can be found in [18].

Theorem 4.25. *A graph $G = (V, E)$ is a Laman graph if and only if for any two different vertices $v, w \in V$, the (multi-)graph on V with edge set $E \cup vw$ is the union of two disjoint spanning trees.*

We do not prove Theorem 4.25 here, instead we show that for a special choice of v and w, there is a straightforward way of dividing $G_{\text{blue}} \cup vw$ into two disjoint spanning trees.

Proposition 4.26. *The multigraph $G'_{blue} := (V, E_{blue} \cup r_1 r_2)$ is the union of two disjoint spanning trees. An analogous assertion holds for G_{red}.*

Proof. We show that $G'_{\text{blue}} = (V, E)$ can be divided into T_{left} and T_{right} where these two are disjoint spanning trees of V. T_{left} is built by taking the left incoming blue edge at each vertex, T_{right} by always taking the right incoming blue edge. Clearly, each edge of G_{blue} is either in T_{left} or in T_{right}. The edge $t_1 t_n$ is contained twice in $E(G'_{\text{blue}})$; we consider the additional copy as directed from t_n to t_1. Thus, this edge is exceptionally directed from the shorter to the longer bar. Recall that we assumed for this subsection that $t_1 = r_1$ and $t_n = r_2$.

As G is maximal, each bar has exactly one incoming edge from the left, except for $B(t_1)$ which has none. Thus, there are $n - 1$ edges in $E(T_{\text{left}})$. Since each edge leads from a longer to a shorter bar, we know that $E(T_{\text{left}})$ does not contain cycles. Therefore T_{left} is a tree. See Figure 4.16 for illustration.

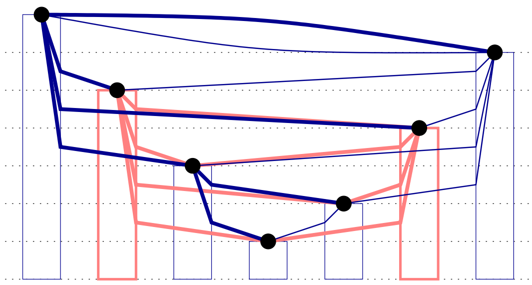

Figure 4.16: T_{left} of G'_{blue} is shown with thick edges.

Almost the same argument holds for T_{right}. Now each bar except for $B(t_n)$ has an incoming edge from the right; for $B(t_1)$, this is the additional edge (t_n, t_1). We have to be a little bit careful when proving that T_{right} is cycle-free: There is one edge in $E(T_{\text{right}})$ leading from a shorter to a longer bar, namely, $(t_n, t_1) = (r_{n-1}, r_n)$. Thus, a t_1-t_n-path in $E(T_{\text{right}})$ would close a cycle. But the only t_1-t_n-path in G_{blue} is the edge (t_1, t_n) – which is contained in $E(T_{\text{left}})$. Therefore T_{right} is a tree as well.

As for G_{red}, we have to incorporate that $V(G_{\text{red}}) = V(G) \setminus \{t_1, t_2\}$. But since the two longest bars representing $V(G_{\text{red}})$ are $B(t_2)$ and $B(t_{n-1})$, the same proof can be used to show that $G'_{\text{red}} := (V, E_{\text{red}} \cup r_3r_4)$ is the union of two disjoint spanning trees. □

This nice result shows that for maximal SB1Vs, 2PLANAR does in fact more than partitioning the edges into two planar graphs: It divides them into (almost) four disjoint spanning trees (in fact, by doubling all edges of the K_4 induced by the longest bars we could obtain four trees spanning all vertices). A priori, it is not clear why this should be possible, even after doubling some edges between the longest bars: For general (multi-)graphs, it is known that every $2k$-edge-connected graph has k edge-disjoint spanning trees (see [11]) – but SB1Vs clearly are not 8-edge-connected.

As a conclusion we point out again that the algorithm 2PLANAR does not only show that the thickness of SB1Vs is bounded by 2, it also reveals the strong structure of SB1Vs, especially in the maximal case.

Conclusion

"Steps are urgently needed to improve visibility, impact and effectiveness."
Javier Solana

While we have answered some problems concerning bar k-visibility graphs, many others are left open, and new ones emerged. We summarize the most intriguing ones here.

We disproved the conjecture of Dean et al. [8] that the tight upper bound on the thickness of bar 1-visibility graphs is 2. Whereas Dean et al. showed an upper bound of 4, we found a bar 1-visibility graph with thickness 3 – which still leaves a gap waiting to be closed. Based on our work we make the following conjecture (which we repeat for emphasis) about the tight bound:

Conjecture 1. *Bar* 1*-visibility graphs have thickness at most* 3*.*

As an intermediate step in the process of understanding bar k-visibility representations and the associated graphs we considered representations by semi bars. We have seen that the strong combinatorial structure of semi bar k-visibility graphs allows us to encode them by a unique permutation. We proved a tight upper bound on the thickness for the case $k = 1$. We also used the structure of semi bar k-visibility graphs to get tight bounds on the maximum number of edges, the chromatic number and the connectivity, and to reconstruct semi bar k-visibility representations of abstract graphs given with a labeled Hamilton cycle.

How can the results on semi bar k-visibility graphs be transferred to general bar k-visibility graphs, e.g. in order to prove Conjecture 1? A first approach might be to extend our results to the intermediate class of bar representations admitting a stabbing line (cf. the introduction to Section 4.6). The bar k-visibility graphs induced by these bar representations are the edge-union of two semi bar k-visiblity graphs and admit an encoding by two permutations.

While the long-term goal of complete characterizing bar k-visibility graph still seems far, the following open questions may serve as starting points for further research.

We showed that semi bar 1-visibility graphs have thickness at most 2 and conjectured (cf. Section 4.6) that this bound also holds for their geometric thickness. How can this be generalized to semi bar k-visibility graphs?

Of course, a result for general k would also be desirable for bar k-visibility graphs. The quadratic function of Theorem 3.11 is presumably not even asymptotically tight as upper bound on the thickness (for $k = 1$ it yields 21, opposed to 3 or 4). What is the smallest such function? Can we bound the geometric thickness of bar k-visibility graphs?

The reconstruction of semi bar k-visibility representations in Section 4.4 requires a maximal graph as input. What if this condition is not fulfilled? What if the additional information of a t-order is not given as input? Also, it is not clear how to use the given construction to effectively count the number of semi bar k-visibility representations of a fixed graph. Is there a structure related to the graph helping us to achieve this, as the dual tree for the case $k = 0$?

The upper bound of $6k + 6$ on the chromatic number of bar k-visibility graphs (cf. Prop. 3.4) merely uses the maximum number of edges. For $k = 0$, the Four Color Theorem shows that this bound is not tight. Is there a better bound for general k?

Hartke, Vandenbussche and Wenger [20] constructed connected $(2k + 2)$-regular bar k-visibility graphs for $k \leq 4$ (see Section 3.5) which are not complete. Can we construct such graphs for $k \geq 5$? Are there d-regular bar k-visibility graphs for $d \geq 2k + 3$ which are connected and non-complete? Hartke et al. also ask for forbidden subgraphs of bar k-visibility graphs apart from triangle-free graphs which have no bar 0-visibility representation (cf. Section 3.6).

In the first paper on bar k-visibility graphs, Dean et al. [8] ask for the largest crossing number and the largest genus of bar k-visibility graphs. Now we can also consider these questions for semi bar k-visibility graphs.

Another way to immediately create a whole bouqet of open questions is to transfer the concept of k-visibility to other variants of visibility graphs, e.g. to rectangle visibility graphs as defined in [3], or to arc- and circle-visibility graphs [21], to name only two of them. We close with this hint to the manifold possibilities of further research on bar k-visibility graphs.

Bibliography

[1] V. B. Alekseev and V. S. Gončakov, *The thickness of an arbitrary complete graph*, Mat. Sbornik **30** (1976), no. 2, 187–202.

[2] Lowell W. Beineke and Frank Harary, *The thickness of the complete graph*, Canadian Journal of Mathematics **17** (1965), 850–859.

[3] Prosenjit Bose, Alice M. Dean, Joan P. Hutchinson, and Thomas C. Shermer, *On rectangle visibility graphs*, Proceedings of Graph Drawing '96, Lecture Notes Comput. Sci., vol. 1353, Springer, 1997, pp. 25–44.

[4] Yi-Wu Chang, Joan P. Hutchinson, Michael S. Jacobson, Jeno Lehel, and Douglas B. West, *The bar visibility number of a graph*, SIAM J. Discret. Math. **18** (2005), no. 3, 462–471.

[5] Maria Chudnovsky, Neil Robertson, Paul Seymour, and Robin Thomas, *The strong perfect graph theorem*, Annals of Mathematics **164** (2006), no. 1, 51–229.

[6] Francisco J. Cobos, Juan C. Dana, Ferran Hurtado, Alberto Márquez, and Felipe Mateos, *On a visibility representation of graphs*, Proceedings of Graph Drawing '95, Lecture Notes Comput. Sci., vol. 1027, Springer, 1995, pp. 152–161.

[7] Derek G. Corneil and Udi Rotics, *On the relationship between clique-width and treewidth*, Proceedings of the Workshop on Graph-Theoretic Concepts in Computer Science '01, Springer, 2001, pp. 78–90.

[8] Alice M. Dean, William Evans, Ellen Gethner, Joshua D. Laison, Mohammad Ali Safari, and William T. Trotter, *Bar k-visibility graphs*, Manuscript, 2005.

[9] ______, *Bar k-visibility graphs: Bounds on the number of edges, chromatic number, and thickness*, Proceedings of Graph Drawing '05, Lecture Notes Comput. Sci., vol. 3843, Springer, 2006, pp. 73–82.

[10] Alice M. Dean, Ellen Gethner, and Joan P. Hutchinson, *Unit bar-visibility layouts of triangulated polygons.*, Proceedings of Graph Drawing '04, Lecture Notes Comput. Sci., vol. 3383, Springer, 2005, pp. 111–121.

[11] Reinhard Diestel, *Graph theory*, second ed., chapter 3.5, Springer, 1999.

[12] ______, *Graph theory*, third ed., Springer, 2005.

[13] Michael B. Dillencourt, David Eppstein, and Daniel S. Hirschberg, *Geometric thickness of complete graphs*, J. Graph Algorithms & Applications **4** (2000), no. 3, 5–17, Special issue for Graph Drawing '98.

[14] Pierre Duchet, Yaya Hamidoune, Michel Las Vergnas, and Henry Meyniel, *Representing a planar graph by vertical lines joining different levels*, Discrete Math. **46** (1983), 319–321.

[15] David Eppstein, *Separating thickness from geometric thickness*, Proceedings of Graph Drawing '02, Lecture Notes Comput. Sci., vol. 2528, Springer, 2002, pp. 150–161.

[16] Shimon Even and Robert E. Tarjan, *Computing an st-numbering*, Theoretical Computer Science **2** (1976), no. 3, 339–344.

[17] Istvan Fary, *On straight-line representations of planar graphs*, Acta Scientiarum Mathematicarum **11** (1948), 229–233.

[18] Stefan Felsner, *Geometric graphs and arrangements*, Vieweg, 2004.

[19] Stefan Felsner and Mareike Massow, *Thickness of bar 1-visibility graphs*, Proceedings of Graph Drawing '06, 2006, to appear.

[20] Stephen G. Hartke, Jennifer Vandenbussche, and Paul Wenger, *Further results on bar k-visibility graphs*, Manuscript, November 2005.

[21] Joan P. Hutchinson, *Arc- and circle-visibility graphs*, Australas. Journal of Combin. **25** (2002), 241–262.

[22] F. Luccio, S. Mazzone, and C. K. Wong, *Visibility graphs*, Prog. naz. teoria degli algoritmi, report 9, University of Pisa, 1983.

[23] ______, *A note on visibility graphs*, Discrete Math. **64** (1987), no. 2-3, 209–219.

[24] Anthony Mansfield, *Determining the thickness of graphs is NP-hard*, Math. Proc. Camb. Phil. Soc. **9** (1983), 9–23.

[25] Petra Mutzel, Thomas Odenthal, and Mark Scharbrodt, *The thickness of graphs: A survey*, Graphs and Combinatorics **14** (1998), 59–73.

[26] R. H. J. M. Otten and J. G. van Wijk, *Graph representations in interactive layout design*, Proceedings IEEE International Symposium on Circuits and Systems, 1978, pp. 914–918.

[27] Neil Robertson, Daniel P. Sanders, Paul D. Seymour, and Robin Thomas, *The four-colour theorem*, Journal of Combinatorial Theory **70** (1997), no. B, 2–44.

[28] Donald J. Rose, *On simple characterizations of k-trees*, Discrete Math. **7** (1974), 317–322.

[29] Richard P. Stanley, *Enumerative combinatorics*, vol. 2, Cambridge University Press, 1999.

[30] Roberto Tamassia and Ioannis G. Tollis, *A unified approach to visibility representations of planar graphs*, Discrete Computational Geometry **1** (1986), 321–341.

[31] William T. Tutte, *The thickness of a graph*, Indag. Math. **25** (1963), 567–577.

[32] Douglas B. West, *Introduction to graph theory*, second ed., Prentice Hall, 2001.

[33] Stephen K. Wismath, *Characterizing bar line-of-sight graphs*, Proceedings of SCG ’85, ACM Press, 1985, pp. 147–152.

Zusammenfassung

Die vorliegende Diplomarbeit beschäftigt sich mit einer erst 2005 eingeführten Klasse von Sichtbarkeitsgraphen, den Balken k-Sichtbarkeitsgraphen. Diese Graphenklasse verallgemeinert Balken-Sichtbarkeitsgraphen. Ein Graph G ist ein Balken-Sichtbarkeitsgraphen, wenn er folgende Balken-Darstellung in der Ebene hat: Die Knoten von G entsprechen paarweise disjunkten horizontalen Geradensegmenten (den *Balken*), und zwei Knoten sind adjazent genau dann, wenn sich die entsprechenden Balken *sehen*. Nun sehen sich zwei Balken, wenn sie sich durch eine vertikale *Sichtlinie* verbinden lassen, die keinen Punkt eines anderen Balken enthält.

Im ersten Kapitel dieser Diplomarbeit werden Balken-Sichtbarkeitsgraphen vorgestellt und verschiedene Variationen von Sichtbarkeit betrachtet. Balken-Sichtbarkeitsgraphen sind in allen diesen Fällen planar. Wir präsentieren die wichtigsten Ergebnisse zu dieser Graphenklasse, insbesondere eine vollständige Charakterisierung von Balken-Sichtbarkeitsgraphen.

In Kapitel 2 stellen wir eine Unterklasse von Balken-Sichtbarkeitsgraphen vor: Wir betrachten nun nur *Semi-Balken*, d.h. , Balken, deren linker Endpunkt die Abszisse 0 hat. Graphen, die eine Darstellung durch Semi Balken erlauben, nennen wir *Semi-Balken-Sichtbarkeitsgraphen*. Auch diese Graphen kann man vollständig charakterisieren, wie wir in Kapitel 2 beweisen. Außerdem zeigen wir, wie man unter bestimmten Voraussetzungen eine Semi-Balken Darstellung eines gegebenen abstrakten Graphen konstruiert.

Die zentrale Graphenklasse dieser Arbeit wird in Kapitel 3 vorgestellt. Wir erweitern hierfür die Definition einer Sichtlinie, so dass sie nun bis zu k Balken schneiden kann. Die hierdurch definierten Balken-k-Sichtbarkeitsgraphen erweisen sich als wesentlich komplexer als die ursprünglichen Balken-Sichtbarkeitsgraphen. Insbesondere sind sie nicht planar. Eingeführt wurde diese Graphenklasse von Dean, Evans, Gethner, Laison, Safari und Trotter in [8]. Sie stellten die Vermutung auf, dass sich alle Balken-1-Sichtbarkeitsgraphen in zwei planare Graphen zerlegen lassen (d.h. sie haben Dicke höchstens 2). Das zentrale Ergebnis dieser Diplomarbeit ist die Widerlegung dieser Vermutung: In Kapitel 3 beschreiben wir eine Konstruktion eines Balken-1-Sichtbarkeitsgraphen, der sich erwiesenermaßen nicht in zwei planare Graphen zerlegen lässt, sondern Dicke 3 hat. – Darüber hinaus präsentieren wir in diesem Kapitel alle bisher bekannten Ergebnisse über Balken-k-Sichtbarkeitsgraphen.

In Kapitel 4 verallgemeinern wir die Definition von Semi-Balken-Sichtbarkeitsgraphen auf Semi-Balken-k-Sichtbarkeitsgraphen. Trotz ihres langen Namens lassen sich diese Graphen durch eine einzige Permutation codieren. Viele Graphen-Probleme können wir dadurch für Semi-Balken-k-Sichtbarkeitsgraphen äußerst befriedigend lösen. Das wichtigste Resultat dieses Kapitels ist ein Algorithmus, der die Kanten eines Semi-Balken-1-Sichtbarkeitsgraphen in zwei planare Teilgraphen aufteilt. Die Dicke dieser Graphen ist daher tatsächlich höchstens 2.

In der Zusammenfassung stellen wir eine Reihe offener Fragen vor, die von vorigen Autoren gestellt wurden oder sich aus dieser Arbeit ergeben.